Identification of Cysteines Involved in *S*-Nitrosylation, *S*-Glutathionylation, and Oxidation to Disulfides in Ryanodine Receptor Type 1*

Paula Aracena-Parks[‡], Sanjeewa A. Goonasekera[§], Charles P. Gilman[‡], Robert T. Dirksen[§], Cecilia Hidalgo[¶], and Susan L. Hamilton[‡1]

From the [‡]Department of Molecular Physiology and Biophysics, Baylor College of Medicine, Houston, Texas 77030, the [§]Department of Pharmacology and Physiology, University of Rochester School of Medicine and Dentistry, Rochester, New York 14642, and [¶]Centro FONDAP de Estudios Moleculares de la Célula and Programa de Biología Celular y Molecular, Instituto de Ciencias Biomédicas, Facultad de Medicina, Universidad de Chile, Santiago 7, Chile

The skeletal muscle Ca^{2+}-release channel (ryanodine receptor type 1 (RyR1)) is a redox sensor, susceptible to reversible *S*-nitrosylation, *S*-glutathionylation, and disulfide oxidation. So far, Cys-3635 remains the only cysteine residue identified as functionally relevant to the redox sensing properties of the channel. We demonstrate that expression of the C3635A-RyR1 mutant in RyR1-null myotubes alters the sensitivity of the ryanodine receptor to activation by voltage, indicating that Cys-3635 is involved in voltage-gated excitation-contraction coupling. However, H_2O_2 treatment of C3635A-RyR1 channels or wild-type RyR1, following their expression in human embryonic kidney cells, enhances [^{3}H]ryanodine binding to the same extent, suggesting that cysteines other than Cys-3635 are responsible for the oxidative enhancement of channel activity. Using a combination of Western blotting and sulfhydryl-directed fluorescent labeling, we found that two large regions of RyR1 (amino acids 1–2401 and 3120–4475), previously shown to be involved in disulfide bond formation, are also major sites of both *S*-nitrosylation and *S*-glutathionylation. Using selective isotope-coded affinity tag labeling of RyR1 and matrix-assisted laser desorption/ionization time-of-flight mass spectroscopy, we identified, out of the 100 cysteines in each RyR1 subunit, 9 that are endogenously modified (Cys-36, Cys-315, Cys-811, Cys-906, Cys-1591, Cys-2326, Cys-2363, Cys-3193, and Cys-3635) and another 3 residues that were only modified with exogenous redox agents (Cys-253, Cys-1040, and Cys-1303). We also identified the types of redox modification each of these cysteines can undergo. In summary, we have identified a discrete subset of cysteines that are likely to be involved in the functional response of RyR1 to different redox modifications (*S*-nitrosylation, *S*-glutathionylation, and oxidation to disulfides).

Ca^{2+}-release channels, also known as ryanodine receptors (RyRs),[2] play crucial roles in several cellular Ca^{2+}-signaling pathways. These channels contribute to muscle contraction, secretion, synaptic plasticity and learning, fecundation, and apoptosis. Consistent with these important roles in cell signaling, RyRs are tightly regulated by a variety of ions and small molecules, protein-protein interactions, and post-translational modifications (for recent reviews see Refs. 1–3).

RyRs, homotetramers with subunits that are >5000 amino acids, are the largest integral membrane proteins reported to date (~2.3 MDa). In rabbit skeletal muscle, each subunit of the type 1 RyR (RyR1; Swiss Prot accession P11716) is comprised of 5037 amino acid residues, of which 100 are cysteines (4). Sulfhydryl reagents, however, modify only a few of these cysteines at physiological pH, which are known as the "hyper-reactive" cysteines (5). Modification of these hyper-reactive cysteine residues has marked effects on RyR1 channel open probability. RyR1 activity is enhanced *in vitro* by molecular oxygen (O_2), superoxide anion ($O_2^{\cdot-}$), hydrogen peroxide (H_2O_2), hydroxyl radical ($OH^{\cdot}$), nitric oxide ($NO^{\cdot}$), nitroxyl (HNO) species, glutathione disulfide (GSSG), and *S*-nitrosoglutathione (GSNO) (6–19). In contrast, the intracellular reducing agent glutathione (GSH) decreases RyR1 activity (10, 14–16, 20). These findings, together with those obtained with exogenous sulfhydryl-modifying agents, have lead to the hypothesis that RyR1 is a cellular redox sensor with a few key redox-sensitive cysteines that modulate the response of the channel to activators and inhibitors (for reviews see Refs. 21–25).

Redox modifications on the sulfur atom of cysteine residues belong to the few reversible redox modifications to take place in cells, making them likely components of the RyR1 redox sensor. Disulfide oxidation, *S*-nitrosylation, and *S*-glutathionylation

* This work was supported by National Institutes of Health Grant AR050503, a Muscular Dystrophy Association grant (to S. L. H.), FONDAP Grant 15600001 (to C. H.), and National Institutes of Health Grant AR44657 (to R. T. D.).

[1] To whom correspondence should be addressed: Dept. of Molecular Physiology and Biophysics, Baylor College of Medicine, One Baylor Plaza, 410B, Houston, TX 77030. Tel.: 713-798-5704; Fax: 713-798-5441; E-mail: susanh@bcm.edu.

[2] The abbreviations used are: RyR, Ca^{2+}-release channels/ryanodine receptor; anti-CysNO, anti-*S*-nitrosocysteine; anti-GSH, anti-glutathione; CBB, Coomassie Brilliant Blue; CHAPS, 3-[(3-cholamidopropyl)dimethylammonio]-1-propanesulfonic acid; CPM, 7-diethylamino-3-(4′-maleimidylphenyl)-4-methylcoumarin; DTT, 2,4-dithiothreitol; EC coupling, excitation-contraction coupling; FKBP12, 12-kDa FK506-binding protein; ICAT, isotope-coded affinity tag; MALDI-TOF, matrix-assisted laser desorption/ionization-time of flight; MOPS, 3-(*N*-morpholino)propanesulfonic acid; NEM, *N*-ethylmaleimide; NOC-12, *N*-ethyl-2-(1-ethyl-2-hydroxy-2-nitrosohydrazino)ethanamine; NOR-3, (±)-(*E*)-ethyl-2-[(*E*)-hydroxyimino]-5-nitro-3-hexenamide; PBS, phosphate-buffered saline; RyR1, type-1 RyR; HEK, human embryonic kidney; SR, sarcoplasmic reticulum.

are the only reversible redox modifications so far described for this channel. Although all three modifications affect RyR1 function and/or channel interaction with accessory proteins, they seem to have different effects on RyR1 function (13, 18, 26–29). Out of the 100 cysteine candidates (4) as targets for these modifications, only Cys-3635 has been clearly identified as functionally relevant for the channel redox sensing properties. This cysteine is within the calmodulin-binding site (30, 31) and can be disulfide-bonded to a cysteine on a neighboring subunit located between amino acids 1 and 2401 (32). It has also been identified as the sole target for $NO^{\bullet}$ at low pO_2, leading to channel activation (33), although this finding has been challenged by other authors (34). In addition, at atmospheric pO_2, other cysteine residues seem to be targets for $NO^{\bullet}$ donors such as *S*-nitrosoglutathione (26). Altogether, it is apparent that Cys-3635 cannot account by itself for the redox sensor within RyR1.

Mass spectrometry is an extremely powerful tool to map post-translational modifications in proteins. In an effort to map redox-sensitive cysteines in RyR1, Voss *et al.* (35) identified a number of RyR1 cysteines susceptible to *S*-alkylation by the maleimide derivative 7-diethylamino-3-(4′-maleimidylphenyl)-4-methylcoumarin (CPM). These cysteines include Cys-1040, Cys-1303, Cys-2436, Cys-2565, Cys-2606, Cys-2611, and Cys-3635. Cysteines that react with CPM may, however, be different from those that are modified by $NO^{\bullet}$ donors, oxidants, and *S*-glutathionylating reagents. The functional consequences of the different modifications may also be dissimilar.

In this study, we found that expression of the RyR1 C3635A mutant in dyspedic (RyR1-null) myotubes restores excitation-contraction coupling with minimal differences with respect to wild-type RyR1. Moreover, samples from HEK cells expressing this mutant show the same H_2O_2-induced activation of [^{3}H]ryanodine binding observed in wild-type expressing cells.

By using mass spectrometry, we set out to identify the cysteine residues in RyR1 subject to reversible redox modifications. Following incubation of SR vesicles with different redox agents, we implemented three approaches as follows: 1) Western blot identification of redox-modified tryptic fragments of RyR1 using modification-specific antibodies; 2) selective reduction of redox-modified cysteines followed by labeling with a fluorescent maleimide to identify modified tryptic fragments of RyR1; and 3) selective reduction of specifically modified cysteines followed by isotope-coded affinity tag (ICAT) labeling, purification of the labeled tryptic peptides, and MALDI-TOF mass spectroscopic identification of the selective ICAT-labeled cysteines. The first two approaches identified regions of RyR1 that are redox-modified (1–2401 and 3120–4475), whereas the third approach identified 12 specific cysteines modified (Cys-36, Cys-253, Cys-315, Cys-811, Cys-906, Cys-1040, Cys-1303, Cys-1591, Cys-2326, Cys-2363, Cys-3193, and Cys-3635), all of which are within the regions identified by the first two approaches. Only three of these residues were identified by their hyper-reactivity with CPM (35). We also found that although *S*-nitrosylation, *S*-glutathionylation, and oxidation to disulfides with exogenous agents modify many of the same residues, a few additional residues undergo selective redox modifications.

To our knowledge, this is the first study to describe and differentially identify cysteine targets for all three types of reversible redox modifications by mass spectrometry. Although the physiological relevance of each individual cysteine residue identified in this work has yet to be defined, this technology has the potential to provide the groundwork for the high throughput identification of candidates for redox modifications.

EXPERIMENTAL PROCEDURES

Reagents—Leupeptin, aprotinin, and pepstatin A were obtained from MP Biomedicals (Aurora, OH). Aminobenzamidine, phenylmethylsulfonyl fluoride, bovine serum albumin, MOPS, EGTA, 2,4-dithiothreitol (DTT), *N*-ethylmaleimide (NEM), soybean trypsin inhibitor, Coomassie Brilliant Blue (CBB), sodium nitrite, and L-ascorbic acid were from Sigma. Analytical grade acetone and glycine were from J. T. Baker Inc. Mercuric chloride was from Amresco (Solon, OH). Glutathione, hydrogen peroxide, (±)-(*E*)-ethyl-2-[(*E*)-hydroxyimino]-5-nitro-3-hexenamide (NOR-3), *N*-ethyl-2-(1-ethyl-2-hydroxy-2-nitrosohydrazino)ethanamine (NOC-12), recombinant glutaredoxin-1 from bacterial origin, and unlabeled 9,21-dehydroryanodine were obtained from EMD Biosciences (San Diego). CHAPS was from Avanti Polar Lipids Inc. (Alabaster, AL). Proteomics grade tosyl phenylalanyl chloromethyl ketone-treated trypsin and FuGENE 6 were from Hoffmann-LaRoche. Immobilon-FL membrane was from Millipore (Billerica, MA). Blocker casein blocking buffer in PBS and tosyl phenylalanyl chloromethyl ketone-treated trypsin were from Pierce. Acrylamide/bisacrylamide solution (30%, 2.6% C), ammonium persulfate, SDS, bromphenol blue, protein assay reagent, and Precision Plus protein standards were from Bio-Rad. Alexa-Fluor 680 C_2-maleimide and all standard cell culture reagents were from Invitrogen. [9,21-^{3}H]Ryanodine (0.2 μCi/ml) was from GE Healthcare. Light and heavy ICAT® cleavable molecules, an avidin cartridge column, and ICAT-cleaving reagents were from Applied Biosystems (Foster City, CA).

Antibodies—Mouse monoclonal anti-glutathione (anti-GSH) antibody was obtained from Virogen (Watertown, MA). Rabbit polyclonal anti-*S*-nitrosocysteine (anti-CysNO) antibody was purchased from Sigma. Mouse monoclonal anti-RyR1 (MAB-925) was from Affinity BioReagents (Golden, CO). Goat polyclonal anti-mouse IgG and C_2-maleimide, both conjugated to Alexa-Fluor 680, were from Invitrogen. Goat polyclonal anti-rabbit IgG and streptavidin, both conjugated to IRDye800, were from Rockland Immunochemicals (Gilbertsville, PA). Rabbit polyclonal anti-RyR1 peptide antibodies were obtained as described previously (36), with the exception of the antibody against the rabbit RyR1 sequence 5029–5037 (a gift by Dr. Paul Allen). For detailed information of peptide sequences recognized by these antipeptide antibodies, see Callaway *et al.* (36), Wu *et al.* (28), and Zhang *et al.* (32).

Animals—Male New Zealand 6-month-old rabbits were euthanized according to the Institutional Animal Care and Use Committee and the Center for Comparative Medicine (Baylor College of Medicine). Rabbit fast-twitch (white) skeletal muscle was dissected from hind limbs and back strap, fast-frozen in liquid nitrogen, and stored at −80 °C up to 6 months.

Sarcoplasmic Reticulum Vesicles Isolation from Rabbit Skeletal Muscle—Heavy SR vesicles were isolated from skeletal muscle as described previously (37). Protein concentration was measured according to Lowry *et al.* (38).

Plasmid Construction—Wild-type rabbit RyR1 and C3635A RyR1 plasmids were created by two rounds of bacterial homologous recombination. The *Escherichia coli* strain pML104/DH10β (a gift from Pumin Zhang) was transformed first with RyR1 in the pMT2 vector (a gift from D. H. MacLennan) and then with a 1200-bp fragment consisting of the C3635A mutation proximal to the tetracycline resistance gene (tet_R) and two flanking regions (~80 bases each) homologous to the wild-type plasmid. First round recombinants were selected by tetracycline resistance on agar plates. Second round recombination occurred when the tet_R bacteria were transformed with a 200-bp fragment consisting of the C3635A mutation flanked by two 80-bp RYR1 homologous regions. Positive recombinants were selected on fusaric acid-agar plates. Recombinations were confirmed by sequencing at the Baylor College of Medicine Sequencing Core facility.

HEK Cell Cultures—HEK 293T cells were maintained in 10% fetal bovine serum, 100 units/ml penicillin, 100 units/ml streptomycin, and 0.25 μg/ml amphotericin B in Dulbecco's modified Eagle's medium. Transfection of C3635A and wild-type RyR1 plasmids was performed with FuGENE 6 in 100-mm TC-treated dishes according to the manufacturer's instructions. The culture medium was supplemented with 800 μg/ml G418 after 24 h to select for stably transfected HEK cells. After 5–7 days in G418, colonies were then grown in 96-well plates from single cells. The presence of expressed wild-type and C3635A RyR1 protein was measured by immunofluorescence with a mouse monoclonal anti-RyR1 antibody (MAB-925). Cell lines were subcloned and subjected to immunofluorescence in this manner three times before being used in experiments. All subsequent cultures were maintained in 500 μg/ml G418, and expression was confirmed by Western blotting.

Microsome Isolation from HEK Cells—Cells were washed twice with cold PBS and centrifuged at 1000 × *g*. Cell pellets were resuspended in a hypotonic buffer (20 mM NaCl, 50 mM MOPS-NaOH at pH 7.4). Following incubation in ice for 10 min, cells were further disrupted by two cycles of freeze-thaw in liquid nitrogen. Cells were homogenized by 10 passages through a 26-gauge needle and centrifuged at 9000 × *g* for 15 min at 4 °C. Supernatants were centrifuged at 100,000 × *g* for 1 h at 4 °C. Pellets (microsomes) were resuspended in a buffer containing 0.3 M sucrose, 0.1 M KCl in 50 mM MOPS-NaOH, pH 7.4. Microsomes were aliquoted, snap-frozen in liquid nitrogen, and stored at −80 °C until use. Protein concentration was measured according to Lowry *et al.* (38).

Treatment with Redox Agents—SR vesicles from rabbit skeletal muscle or microsomes from HEK cells (1 mg/ml) were incubated with each redox agent at the following concentrations: 250 μM NOR-3, 250 μM NOC-12, 4 mM GSH plus 100 μM H_2O_2, 5 mM H_2O_2, or 250 μM GSNO. Incubation was carried out in the absence of Mg^{2+} at *p*Ca 5, in 300 mM NaCl, 50 mM MOPS-NaOH buffer (pH 7.4) for 30 min at 23 °C. Following incubation, redox agents were washed by centrifugation at 100,000 × *g* for 45 min (4 °C), and vesicles were resuspended to 10 mg/ml in 300 mM NaCl, 50 mM MOPS-NaOH (pH 7.4).

Equilibrium [^{3}H]Ryanodine Binding—Following incubation with different redox agents, samples (1 mg/ml) were washed by centrifugation at 100,000 × *g* for 30 min. Resuspended membranes (10 μg per reaction) were incubated with increasing concentrations (0.75–50 nM) of [^{3}H]ryanodine in a buffer solution containing 1.2 mM $CaCl_2$, 1 mM EGTA, 300 mM NaCl, 0.1 mg/ml bovine serum albumin, 0.1% CHAPS, and 50 mM MOPS (NaOH), pH 7.2, for 16–18 h at 23 °C. Nonspecific activity was evaluated in the additional presence of 1 μM unlabeled ryanodine. Separation of free from bound ligand was attained by vacuum filtration through GF/F filters (Whatman). Filters were washed five times with 3 ml of a buffer containing 0.1 mM $CaCl_2$, 300 mM NaCl, and 50 mM MOPS (NaOH), pH 7.2. Radioactivity associated to filters was assessed by liquid scintillation counting.

Preparation and Microinjection of Myotubes—Myoblasts obtained from neonatal RyR1-null (dyspedic) mice were used to generate primary cultures of skeletal myotubes. 5–7 days after plating, individual myotube nuclei were microinjected with cDNAs encoding CD8 (0.1 μg/μl) and either wild-type RyR1 or C3635A (0.5 μg/μl). Injected myotubes were identified 3 days later following incubation and decoration with CD8 antibody-coated beads.

Measurement of Ca^{2+} Currents and Ca^{2+} Transients—L-type Ca^{2+} currents (L-currents) and intracellular Ca^{2+} transients were recorded under conditions of minimal disruption of the intracellular environment using the perforated patch clamp technique (39). Expressing myotubes were first loaded for 20 min at 37 °C with fluo-4 AM. The perforated patch clamp technique was then used in fluo-4-loaded myotubes, with an internal pipette solution containing (in mM) the following: 145 cesium aspartate, 0.1 Cs_2-EGTA, 1.2 $MgCl_2$, 10 HEPES (pH 7.4), and 240 μg/ml amphotericin B and an external recording solution containing (in mM) the following: 145 tetraethylammonium-Cl, 10 $CaCl_2$, and 10 HEPES (pH 7.4). Peak L-current magnitude was normalized to total cell capacitance (pA/pF), plotted as a function of membrane potential (V_m), and fitted according to Equation 1,

$$I = G_{max} \times (V_m - V_{rev})/(1 + \exp((V_{G1/2} - V_m)/k_G)) \quad \text{(Eq. 1)}$$

where G_{max} is the maximal L-channel conductance; V_m is the test potential; $V_{G½}$ is the voltage of half-maximal activation of G_{max}; V_{rev} is the extrapolated reversal potential, and k_G is a slope factor. Ca^{2+} transients recorded during each test pulse were expressed as $\Delta F/F$, where F represents base-line fluorescence and ΔF represents the fluorescence change from base line. Maximum voltage-gated Ca^{2+} release ($(\Delta F/F)_{max}$) was estimated by fitting the data according to Equation 2,

$$\Delta F/F = (\Delta F/F)_{max}/\{1 + \exp((V_{F1/2} - V_m)/k_F)\} \quad \text{(Eq. 2)}$$

where $(\Delta F/F)_{max}$ is the maximal fluorescence change; V_m is the test potential; $V_{F½}$ is the voltage of half-maximal activation of $(\Delta F/F)_{max}$, and k_F is a slope factor. Pooled current voltage and fluorescence voltage data are expressed as mean ± S.E.

Generation and Purification of the RyR1 Major Tryptic Fragments Complex—Treated or control (buffer only) SR vesicles (10 mg/ml) were incubated with tosyl phenylalanyl chloromethyl ketone-treated trypsin in a 1:1000 of enzyme/protein ratio for 2 min at 37 °C in 300 mM NaCl, 1 mM EGTA, and 50 mM MOPS-NaOH (pH 7.4). The digestion was stopped by the addi-

tion of 10-fold excess of soybean trypsin inhibitor. Samples were then solubilized with 2% CHAPS (final concentration) for 30 min on ice, in the same buffer. Afterward, samples were loaded onto a 5–20% linear sucrose gradient in 0.4% CHAPS, 300 mM NaCl, and 50 mM MOPS-NaOH (pH 7.4). Gradients were centrifuged at 105,000 × *g* for 17 h, and 1.25-ml fractions were collected. RyR1 major tryptic fragment complex purification was assessed by electrophoresis of each fraction under nonreducing conditions, as described below, followed by CBB staining. Routinely, the RyR1 major tryptic fragment complex migrated to the bottom of the gradient, between fractions 4 and 10 out of 30–35. Fractions containing RyR1 tryptic fragments were pooled and concentrated using Amicon Ultra filter tubes (Millipore) with a cutoff of 10,000 Da. Total protein concentration was determined by the Lowry method (38).

Western Blots—Fragments were subjected to SDS-PAGE under nonreducing conditions. In brief, samples were denatured in a mixture containing (in final concentrations) the following: 5 mM NEM, 2% SDS, 10% glycerol, and 0.001% bromphenol blue in 62 mM Tris-HCl buffer (pH 6.8) for 30 min at 65 °C. Five micrograms of each sample were electrophoresed using a 4% stacking, 7.5% resolving gel system, according to Laemmli (40), for 30 min at 80 V plus 2 h at 120 V (4 °C). Electrophoresed proteins were transferred onto Immobilon-FL membranes overnight (16–17 h) at 22 V and 4 °C. Afterward, membranes were blocked with casein-PBS blocking buffer for 30 min under constant rocking at 23 °C. Membranes were then incubated with a mixture containing rabbit polyclonal anti-CysNO antibody (1:1000 dilution in casein-PBS blocking buffer) and mouse monoclonal anti-GSH antibody (1:1000 dilution in casein-PBS blocking buffer) for 1 h at 23 °C, under constant rocking. Membranes were then washed four times with PBS-T for 5 min prior to incubation with a mixture of goat polyclonal anti-mouse and anti-rabbit IgGs, conjugated to Alexa-Fluor 680 IR800Dye, respectively (1:5000 dilution each in casein-PBS blocking buffer). After washing membranes two times with PBS-T for 5 min each plus two times with PBS for 5 min each, membranes were scanned for fluorescence emission at 700 and 800 nm, using an Odyssey® infrared imaging system (Li-Cor Biosciences, Lincoln, NE). Signals for each wavelength are rendered as red and green, respectively. Identification of fragments was performed in parallel Western blots using rabbit polyclonal anti-RyR1 peptide antibodies 001, 416, 2391, 4198, and 5029 (see Refs. 28, 32, and 36 for details of RyR1 sequences recognized) and Edman sequencing (Protein Core of Baylor College of Medicine). As a final step, membranes were stained with a solution containing 0.001% CBB, 50% methanol, and 10% acetic acid in water. Membranes were then scanned in a FluoroMax® scanner (Bio-Rad), using the colorimetric option. Densitometric analysis of fluorescent signals was performed using the Odyssey scanner software; analysis of the CBB staining densities was performed in the blotted membranes using Quantity One® software (Bio-Rad). For quantification, results are shown as a ratio of fluorescence/CBB staining.

Acetone Precipitation—In the following protocols, several steps describing selective reduction of RyR1 fragments involved stopping reactions and washing reagents through acetone precipitation, which was accomplished by adding 2 volumes of pre-chilled acetone (−20 °C) and mixing by inversion. Protein was allowed to precipitate for at least 30 min at −20 °C, and samples were then centrifuged at 5,000 × *g* for 10 min. The supernatant was discarded, and pelleted fragments were redissolved in 0.2 ml of 0.1% SDS and 50 mM Tris-HCl buffer (pH 8.0).

Selective Reduction of S-Nitrosylated Residues—One hundred micrograms of RyR1 fragments (0.5 mg/ml) were incubated with 5 mM NEM for 30 min on ice. Following acetone precipitation, redissolved fragments were incubated with or without 0.1 mM $HgCl_2$ for 30 min on ice. Samples were acetone-precipitated, and redissolved fragments were incubated with 1 mM ascorbic acid for 30 min on ice. After acetone precipitation, samples were labeled with either C_2-maleimide-conjugated Alexa-Fluor 680 (C_2M) or ICAT®-cleavable molecules, as described below.

Selective Reduction of S-Nitrosylated and/or S-Glutathionylated Residues—One hundred micrograms of RyR1 fragments (0.5 mg/ml) were incubated with 5 mM NEM for 30 min on ice. Following acetone precipitation, redissolved fragments were incubated with 1 unit/ml recombinant glutaredoxin and 0.5 mM GSH for 5 min at 37 °C. In some experiments, samples were then acetone-precipitated, and redissolved fragments were incubated with or without 0.1 mM $HgCl_2$ for 30 min on ice before reduction with glutaredoxin. Following the final acetone-precipitation, samples were labeled with either C_2-maleimide conjugated with Alexa-Fluor 680 or ICAT® cleavable molecules, as described below.

Selective Reduction of Disulfide Cross-linked Residues—One hundred micrograms of RyR1 fragments (0.5 mg/ml) were incubated with 5 mM NEM for 30 min on ice. Samples were acetone-precipitated, and redissolved fragments were incubated with 1 unit/ml recombinant glutaredoxin and 0.5 mM GSH for 5 min at 37 °C. Samples were acetone-precipitated one more time, and redissolved fragments were incubated with 1 mM NEM for 30 min on ice. After acetone precipitation, redissolved fragments were incubated with 1 mM DTT for 30 min on ice. Samples were acetone-precipitated one final time, and redissolved fragments were incubated with either C_2-maleimide conjugated to Alexa-Fluor 680 or ICAT®-cleavable molecules, as described below.

C_2-Maleimide Labeling and Analysis—Selectively reduced samples (0.5 mg/ml total protein) were incubated with 5 μM C_2-maleimide conjugated to Alexa-Fluor 680 for 30 min on ice. Samples were acetone-precipitated, and fragments were redissolved directly in reducing Laemmli denaturing buffer, consisting of 25 mM DTT, 2% SDS, 10% glycerol, and 0.001% bromphenol blue in 62 mM Tris-HCl buffer (pH 6.8). Following denaturation for 30 min at 65 °C, samples were electrophoresed and transferred to Immobilon-FL as described above. The transfers were scanned for fluorescence emission at 700 nm, using the Odyssey infrared imaging system. Gels were then stained with a solution containing 0.001% CBB, 10% methanol, and 10% acetic acid in water, and scanned in the FluoroMax Scanner, using the gel imaging option.

ICAT Labeling and Analysis—Selectively reduced samples (0.1 mg of total protein) were incubated with 1 unit of either heavy or light ICAT®-cleavable molecules (Applied Biosystems) according to the manufacturer's directions. Labeled fragments were acetone-precipitated and redissolved; light and

heavy ICAT-labeled samples were pooled together in a 1:1 ratio. Mixtures were then extensively trypsinized with 20 μg of proteomics grade tosyl phenylalanyl chloromethyl ketone-treated trypsin for at least 16 h at 37 °C. ICAT-labeled tryptic peptides were purified using an avidin cartridge (Applied Biosystems), following the manufacturer's directions. Cleaved peptides were vacuum-dried and analyzed by MALDI-TOF spectrometry, at the Protein Core of Baylor College of Medicine or at Proteomics Research Services, Inc. (Ann Arbor, MI).

Statistical Analyses—Densitometric analyses were performed by analysis of variance, using GraphPad Prism®, version 4.0. Differences in the means were considered significant with $p < 0.05$.

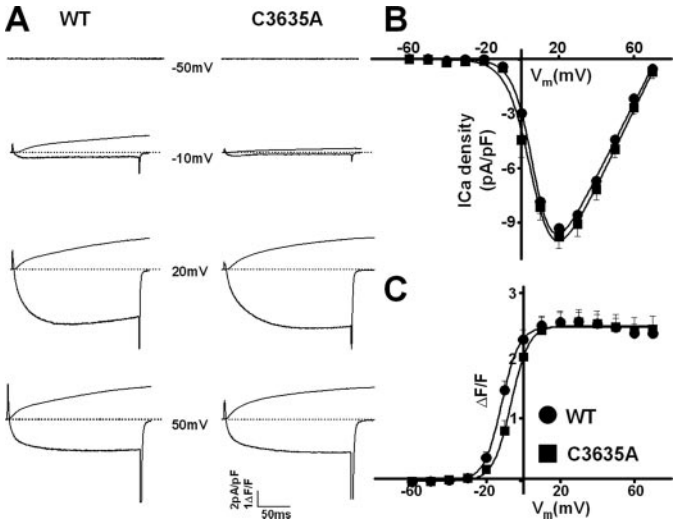

FIGURE 1. **Cys-3635 influences voltage sensor activation of Ca^{2+} release.** Patch clamp experiments were performed in dyspedic myotube cultures, as detailed under "Experimental Procedures." *A,* representative L-type Ca^{2+} currents (*lower traces*) and intracellular Ca^{2+} transients (*upper traces*) recorded in response to 200-ms depolarizations to the indicated potentials in dyspedic myotubes expressing either wild type (*WT*) RyR1 (*left*) or C3635A (*right*). *B* and *C*, voltage dependence of peak L-currents (*B*) and intracellular Ca^{2+} transients (*C*) in wild type (*closed circles*) and C3635A-expressing (*closed squares*) myotubes. Voltage-gated Ca^{2+} release was significantly ($p < 0.01$) shifted to more depolarized potentials in C3635A-expressing myotubes ($V_{F½}$ was -11.8 ± 1.1 and -6.2 ± 1.3 mV in wild type- and C3635A-expressing myotubes, respectively).

RESULTS

Functional Relevance of Cys-3635 in Excitation-Contraction Coupling and in the RyR1 Redox Sensor—Cys-3635 is the only cysteine that has been examined and suggested to be a part of the redox sensor of RyR1. This residue is within the CaM-binding site of RyR1 (30) and can be disulfide-bonded to a neighboring cysteine (32). It also has been suggested as the only target for *S*-nitrosylation by NO• at low pO_2 (33). Although Cys-3635 is likely to play an important role in RyR1 redox sensing, the available evidence suggests that other cysteines are also involved. To evaluate the importance of Cys-3635 in EC coupling, we substituted an alanine residue for Cys-3635 and examined the effects of this mutation on the bi-directional coupling between DHPR-RyR1 following expression in RyR1-null (dyspedic) myotubes. Expression of wild-type RyR1 in dyspedic myotubes restores both robust L-current density (retrograde coupling; Fig. 1, *A* and *B*) and voltage-gated Ca^{2+} release (orthograde coupling; Fig. 1, *A* and *C*), which are absent in naive dyspedic myotubes (41). Expression of C3635A in dyspedic myotubes also fully restored maximal L-current density. The G_{max} value was 210 ± 15 and 208 ± 16 nS/nF in wild-type- and C3635A-expressing myotubes, respectively; the Ca^{2+} transient magnitude $(\Delta F/F)_{max}$ was 2.5 ± 0.1 and 2.5 ± 0.2 in wild-type- and C3635A-expressing myotubes, respectively. The voltage dependence of Ca^{2+} release in C3635A-expressing myotubes, however, was significantly ($p < 0.01$) shifted to more depolarized potentials ($V_{F½}$ was -11.8 ± 1.1 and -6.2 ± 1.3 mV in wild-type- and C3635A-expressing myotubes, respectively). The shift is best seen by comparing Ca^{2+} release at the −10 mV test potential (Fig. 1, *A* and *C*). These results indicate that Cys-3635, possibly due its ability to be redox-modulated, influences RyR1 sensitivity to activation by the voltage sensor during EC coupling.

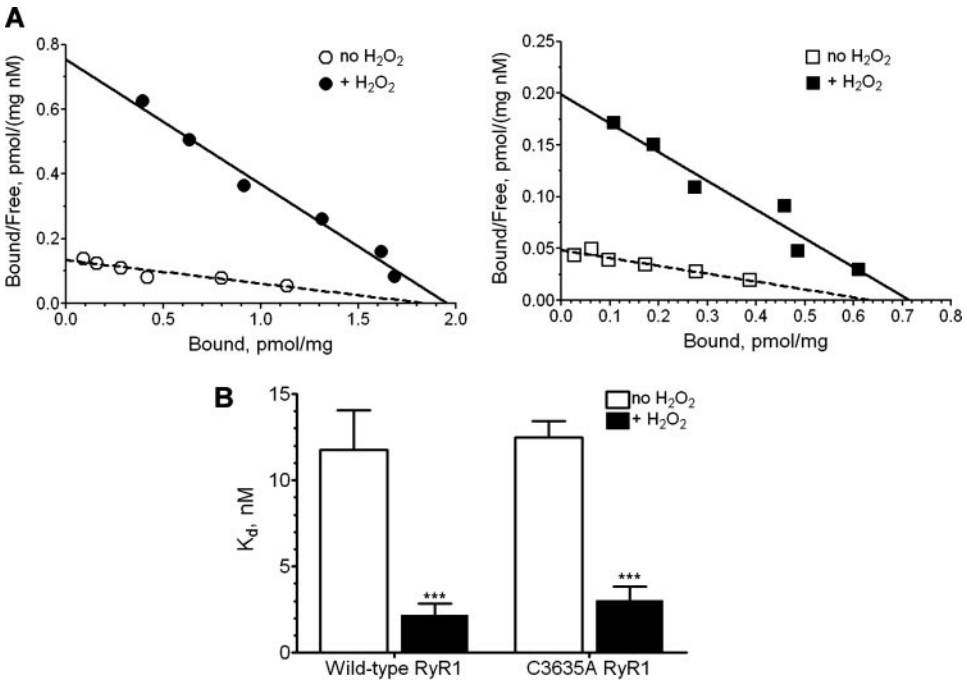

FIGURE 2. **Cys-3635 does not influence activation of [^{3}H]ryanodine by H_2O_2.** *A,* representative Scatchard plots obtained from equilibrium [^{3}H]ryanodine bindings, following incubation of microsomes from HEK cells expressing either wild-type (*circles, left panel*) or C3635A mutant RyR1 (*squares, right panel*) with 5 mM H_2O_2 for 30 min at 23 °C (*closed symbols*) or buffer (*open symbols*), as detailed under "Experimental Procedures." *B,* K_d values obtained from analyses as in *A* are presented as mean ± S.D. of at least three independent experiments. *** indicates significant difference compared with wild-type RyR1-expressing HEK cells (analysis of variance).

Incubation of SR vesicles in *in vitro* preparations with H_2O_2 leads to RyR1 activation as assessed by single channel recordings and [^{3}H]ryanodine binding (27, 28). This activation is thought to be the

consequence of disulfide oxidation of the channel protein. Because one of the candidates for this disulfide cross-link is Cys-3635, we examined the effects of 5 mM H_2O_2 (10 min at 23 °C) on [^{3}H]ryanodine binding to microsomes obtained from HEK cells expressing wild type or a C3635A mutant of RyR1. As shown in Fig. 2 treatment with H_2O_2 increases the apparent affinity for [^{3}H]ryanodine in both wild type and C3635A-transfected HEK cells (Fig. 2*A*). The decrease in apparent K_d for [^{3}H]ryanodine (summarized in Fig. 2*B*) is the same for both samples ($p > 0.05$). Ryanodine binds primarily to the open state of the channel and increases in its apparent affinity are correlated to increased channel activity (42). These data indicate that oxidation of Cys-3635 is not likely to be responsible for the ability of H_2O_2 to enhance channel activity. Our next goal was to identify other cysteines in the RyR1 protein involved in redox modulation of RyR1. Because RyR1 is functionally modified by disulfide oxidation, *S*-nitrosylation, and *S*-glutathionylation, we developed a strategy to identify cysteines with all three types of modifications occurring either endogenously or after treatment with specific redox agents.

Identification of RyR1 Tryptic Fragments That Are Either Endogenously or Spontaneously Redox-modified in RyR1—RyR1 has 100 cysteines, and our goal was to identify targets of reversible redox modifications. To accomplish this goal we first identified large tryptic fragments that were redox-modified as isolated (either endogenously or during purification). Unreduced SR membranes were first digested with trypsin using conditions that cleave RyR1 at 7–9 sites (28, 30, 32, 36). Because RyR1 fragments remain associated, they can be purified as a rapidly sedimenting complex on sucrose gradients (32, 36). Tryptic fragments of RyR1 that were redox-modified were identified using two different approaches as follows: 1) Western blotting with antibodies to detect *S*-nitrosylation (anti-nitrosocysteine, anti-CysNO) or *S*-glutathionylation (anti-glutathione, anti-GSH); and 2) labeling of selectively reduced cysteine residues with a fluorescent maleimide.

Tryptic digestion of RyR1 generates 16–18 fragments in SDS gels, of which 12 are seen in 7.5% resolving Laemmli gels (Fig. 3). All of the fragments have been identified previously by N-terminal Edman sequencing (28, 32). The identity of these bands was confirmed in this study, again by Edman sequencing of the bands in reduced SDS-polyacrylamide gels. For simplicity, the bands were renumbered in this study and do not necessarily correspond to the numbered bands in our previous studies (28, 32, 36). In this study we are attempting to identify bands that are modified by *S*-nitrosylation, *S*-glutathionylation, and oxidation to disulfides. RyR1 forms intersubunit disulfides, both spontaneously and after treatment with diamide or H_2O_2 (27, 28). Our previous study demonstrated that the intersubunit disulfides involved Cys-3635 (found in fragments 1, 2, 4, and 7) and, as yet unidentified, cysteines between amino acids 2000 and 2401, a sequence found within fragments 5 and 6 in this study (32). Because redox modifications are readily reversed by DTT, the gels used in this study were of necessity unreduced and hence were complicated to some extent by spontaneous disulfide bond formation between the above fragments. This feature is illustrated by the difference in the banding pattern of the samples electrophoresed in the presence and absence of

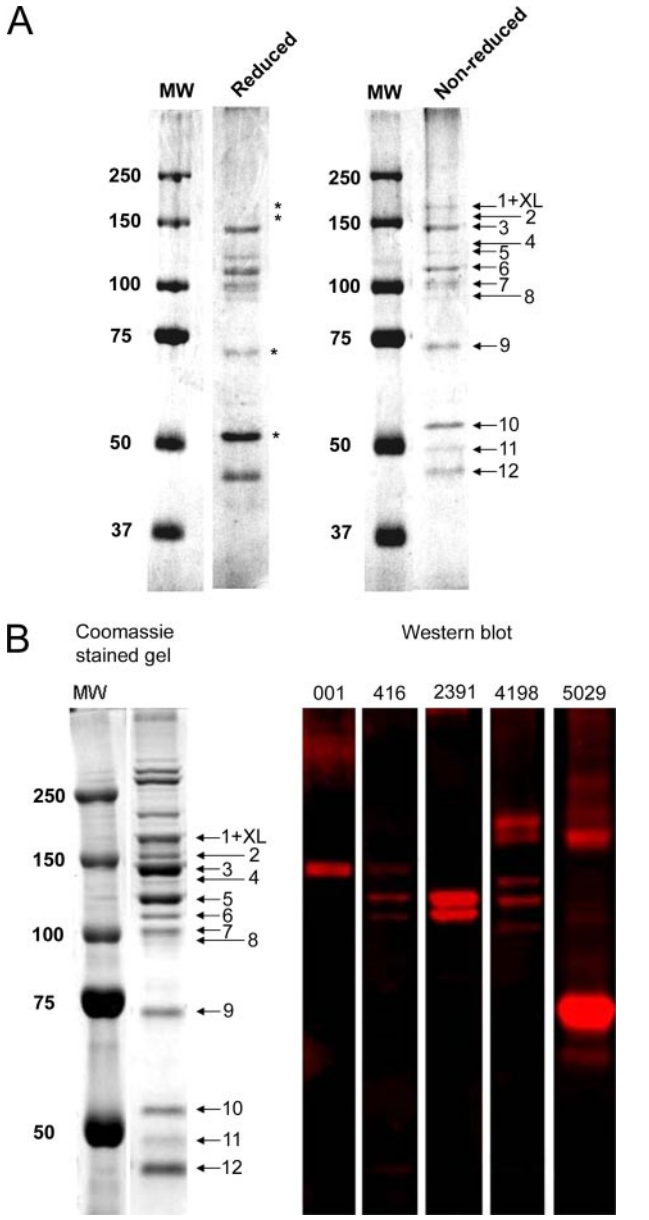

FIGURE 3. **Identification of RyR1 major tryptic fragments.** RyR1 major tryptic complex was prepared and isolated as described under "Experimental Procedures" and electrophoresed under reducing or nonreducing conditions. *A*, representative images ($n = 3$) of reduced (*left*) and nonreduced (*right*) samples. *Stars* indicate differences found between these conditions. *B*, following transfer of RyR1 tryptic fragments (nonreduced samples) to Immobilon-FL membranes, Western blotting was performed using rabbit polyclonal anti-RYR1 peptide antibodies (designated 001, 416, 2391, 4198, and 5029). Information of these antibodies can be found in Refs. 28, 32, and 36. Blots were probed with a goat polyclonal anti-rabbit IgG conjugated to IR700Dye and scanned using a Li-Cor Odyssey Infrared imaging system, using the 700 nm excitation wavelength; finally, membranes were stained with CBB, as described under "Experimental Procedures." A representative image ($n = 2$) of the CB-stained gel (*left*) and fluorescence scan (*right*) is shown. *Numbers* on the *left* indicate molecular mass standards in kDa, and *numbers* on the *right* indicate the identity of tryptic fragments, using the numbering shown in Table 1. *1+XL* indicates the presence of fragment 1 plus a disulfide cross-link product.

DTT (Fig. 3*A*). To overcome possible uncertainties in the identification of redox-modified bands, because of the presence of cross-linked fragments, all assignments were confirmed by MALDI mass spectroscopy. The major consequence of the presence of these cross-linked bands, which overlap bands 1

TABLE 1

Identification of RyR1 major tryptic fragments

SR vesicles were subjected to limited proteolysis, and the RyR1 major tryptic complex was isolated as described under "Experimental Procedures." Tryptic fragments were identified by antibody recognition in nonreducing gels and N-terminal Edman sequencing of reduced samples. Relative molecular mass was obtained from nonreducing SDS-PAGE analysis. 1+XL indicates the presence of fragment 1 plus a disulfide cross-linked product with the same molecular mass when samples are run under nonreducing conditions.

Fragment	N-terminal sequence	Antibody recognition	Residues encompassed	Apparent mass
				kDa
1+XL	TQVKGVGQNL	4198, 5029	3120–5037	179
2	TQVKGVGQNL	4198	3120–4475	163
3	Blocked	001, 426	1–1509	154
4	TQVKGVGQNL	4198	3120-?	146
5	AAMMTQPPAT	2391	1396–2401	133
6	ISHTDLVIGC	2391	1509–2401	124
7	AVVACFRMTP	4198	3631–4475	113
8	GSGPPAGPAL		426–1396	107
9	KLGVDGEEEE	5029	4476–5037	77
10			SERCA1	48
11			SERCA1	41
12	RREHFGEEPP	2840	2402–2840	36

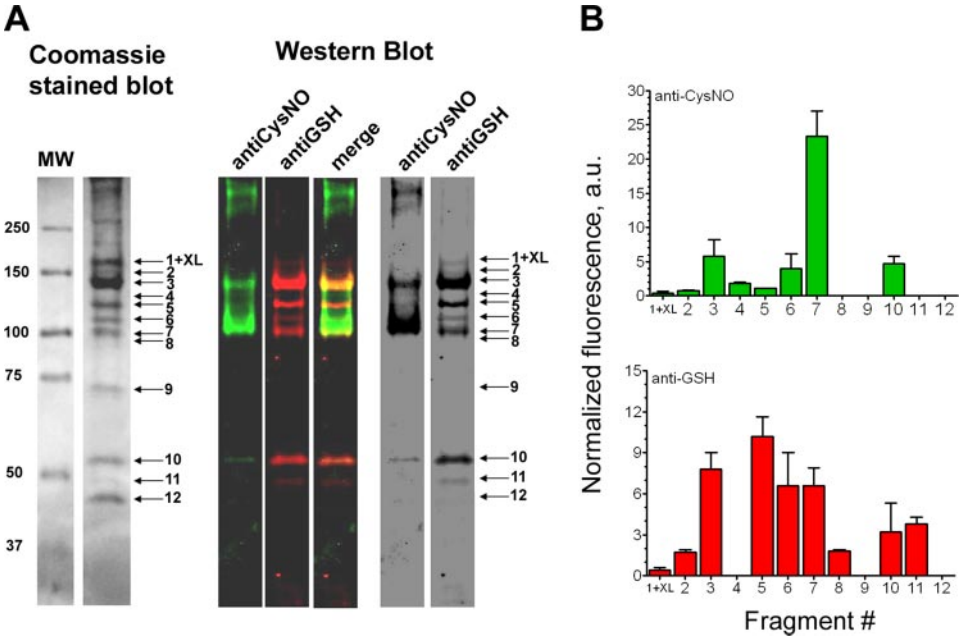

FIGURE 4. **Endogenous redox modifications of RyR1 map to regions 1–2401 and 3631–4475.** RyR1 major tryptic fragments were isolated as described under "Experimental Procedures" and electrophoresed under nonreducing conditions. Following transfer of RyR1 tryptic fragments to Immobilon-FL membranes, Western blotting was performed using mouse monoclonal anti-glutathione (anti-GSH) and rabbit polyclonal anti-nitrosocysteine (anti-CysNO) antibodies. Blots were probed with a mixture of goat polyclonal anti-mouse IgG conjugated to Alexa-Fluor 680 and goat polyclonal anti-rabbit IgG conjugated to IR800Dye and scanned using a Li-Cor Odyssey Infrared imaging system, using 700 and 800 nm excitation wavelengths. Following this analysis, the transfer membranes were stained with CBB, as described under "Experimental Procedures." *A,* representative image ($n = 7$) of the CBB-stained gel (*left*), CBB-stained blot (*center*), and fluorescence scan (*right*); *green* and *red* signals correspond to the detection of anti-CysNO and anti-GSH, respectively, whereas a *yellow* signal indicates merging of both signals. *Numbers* on the *left* indicate molecular mass standards in kDa, and *numbers* on the *right* indicate the identity of tryptic fragments, using the numbering shown in Table 1. *1+XL* indicates the presence of fragment 1 plus a disulfide cross-link product. *B,* densitometric analysis of anti-CysNO (*green bars, top panel*) or anti-GSH (*red bars, bottom panel*) signals from images as in *A*; values correspond to mean ± S.D. ($n = 7$) of fluorescent signals normalized to CBB staining (arbitrary units). *a.u.*, arbitrary units.

and 2 is an underestimation of other redox modifications of bands 1 and 2. Fragment identity in the unreduced gels was also confirmed by antibody recognition with specific anti-RyR1 antibodies (Fig. 3*B*, *right panel*). These results are summarized in Table 1.

Western blot analysis of the purified fragments to detect endogenous modifications (Fig. 4*A*, *right panel*) showed two major bands (fragments 3 and 7) and two minor bands (fragments 2 and 10) recognized by the anti-CysNO antibody, whereas one major band (fragment 3) and six minor bands (fragments 2, 5, 6, 7, 10, and 11) were recognized by the anti-GSH antibody. Densitometric analysis of these bands, normalized to the optical density of the CBB stain of each band (Fig. 4*B*), shows that endogenous *S*-nitrosylation (*top panel*) is mainly associated with fragment 7 (residues 3631–4475) and fragment 3 (residues 1–1509). Endogenous *S*-glutathionylation (Fig. 4*B*, *bottom panel*) is primarily associated with fragments 3 and 6 (residues 1–1509 and 1509–2401, respectively). Significant *S*-glutathionylation was also detected in fragments 2, 5, and 7 (residues 3120–4475, 1396–2401, and 3631–4475, respectively). Neither the anti-CysNO nor the anti-GSH antibodies detected fragments 1 (residues 3120–5037), 8 (residues 426–1396), 9 (residues 4476–5037), or 12 (residues 2402–2840). Our results are in apparent discrepancy because fragments 1 and 8 should be recognized by the antibodies as fragments 3, 5, 6, and 7 are. As mentioned above, fragment 1 co-migrates with a disulfide cross-linked product (named 1+XL throughout this study) under nonreducing conditions, leading to the overestimation of fragment 1 content (assessed by CBB staining) and, thus, underestimation of the normalized antibody recognition. The amount of fragment 8 is below the detection limit of our antibody. Taken together, these findings strongly suggest that endogenous redox modifications on the RyR1 protein are confined to two large regions (amino acids 1–2401 and 3631–4475).

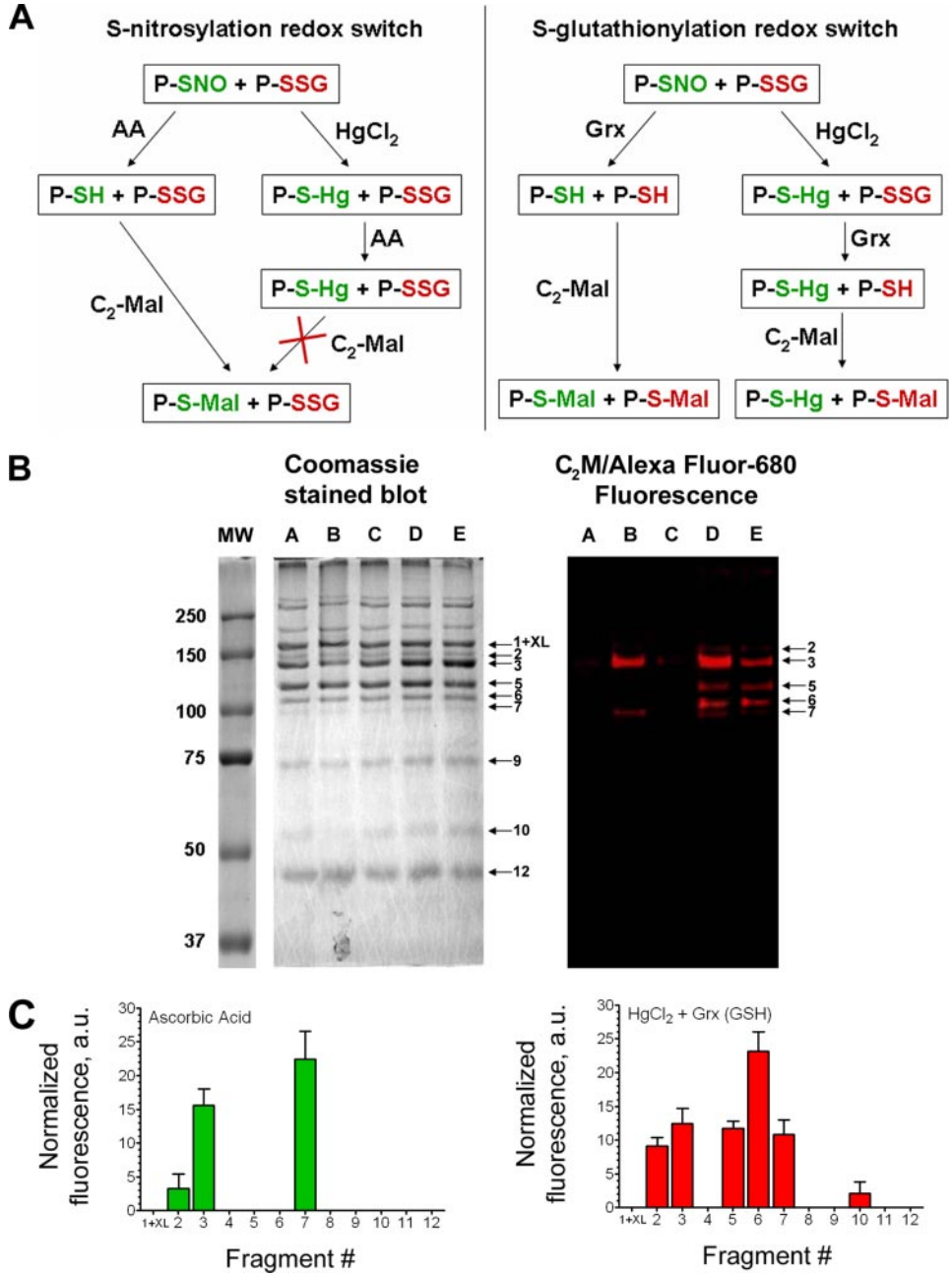

FIGURE 5. **Selective labeling of RyR1 major tryptic fragments with C_2-maleimide.** Endogenously redox-modified RyR1 tryptic fragments were subjected to selective reduction using the redox switches depicted in *A* (see details under "Experimental Procedures"). Ascorbate, glutaredoxin, and C_2-maleimide (*C_2-Mal*) stand for ascorbate, glutaredoxin, and C_2-maleimide probe, respectively. Samples were electrophoresed in a Laemmli system under reducing conditions, and proteins were transferred to an Immobilon-FL membrane. Following analysis in the Odyssey Infrared scanner using the 700 nm excitation wavelength, membranes were stained with CBB. *B,* representative images ($n > 2$) of a CBB-stained blot (*left*) and a fluorescence scan at 700 nm (*right*) are presented. *Numbers* on the *left* correspond to standard molecular masses (in kDa); *numbers* on the *right* correspond to fragment numbering as described in Table 1. *1+XL* indicates the presence of fragment 1 plus a disulfide cross-link product. *Lane A,* NEM-blocked fragments; *lane B,* ascorbate-reduced fragments; *lane C,* fragments treated with $HgCl_2$ followed by ascorbate reduction; *lane D,* glutaredoxin-reduced fragments; *lane E,* fragments treated with $HgCl_2$ followed by glutaredoxin reduction. *C,* densitometric analysis of C_2-maleimide signals after selective reduction with ascorbic acid only (*lane B, top panel*) or $HgCl_2$ treatment followed by reduction with glutaredoxin (*lane E, bottom panel*); values correspond to mean ± S.D. ($n > 2$) of fluorescent signals normalized to CBB staining (*a.u.,* arbitrary units).

cent maleimide (C_2M). This selective reduction takes advantage of the redox switch systems developed by Jaffrey and Snyder (43) and Lind *et al.* (44). RyR1 was digested with trypsin and purified as described above. Unmodified cysteine residues were blocked using 5 mM NEM. Successful alkylation of all unmodified cysteines was demonstrated by the inability of the maleimide probe to label any of the fragments treated with NEM (Fig. 5*B*, *right panel, lane A*). Ascorbate reverses *S*-nitrosylation without reversing either *S*-glutathionylation or disulfide bond formation (43). Ascorbate treatment should convert *S*-nitrosylated residues to reduced cysteine residues, allowing their subsequent reaction with the C_2 fluorescent maleimide (Fig. 5*B*, *right panel, lane B*). Disulfide-bonded higher molecular weight complexes, known to arise from oxidation (32), were not reduced by this treatment (not shown). To confirm the selectivity of the ascorbate treatment, prior to incubation with C_2M, we incubated the samples with mercuric chloride, an agent that displaces the NO$^{\bullet}$ group from *S*-nitrosylated residues and modifies them to prevent further reaction (45). As shown in Fig. 5*B* (*right panel, lane C*), incubation with mercuric chloride completely blocked labeling by C_2M.

Glutaredoxin selectively reduces *S*-glutathionylated cysteines (46). Although there are reports suggesting that this enzyme is also capable of reducing *S*-nitrosylated residues (47, 48), it is not thought to reduce disulfides (49). We treated the endogenously/spontaneously modified, NEM-alkylated proteolytic RyR1 complexes with glutaredoxin 1 and found that several additional fragments were labeled with the maleimide probe compared with those labeled after treatment with ascorbate (compare Fig. 5*B*, *right panel, lanes D* and *B*). To determine whether glutaredoxin also reduced the *S*-nitrosylated cysteines, we pretreated the samples with mercuric chloride, blocking the *S*-nitrosylated cysteines and leaving available for reaction only those cysteines that are *S*-glutathionylated

Our second approach (detailed under "Experimental Procedures" and summarized in the diagram shown in Fig. 5*A*) involved the selective reduction of *S*-nitrosylated and *S*-glutathionylated cysteines, followed by their labeling with a fluores-

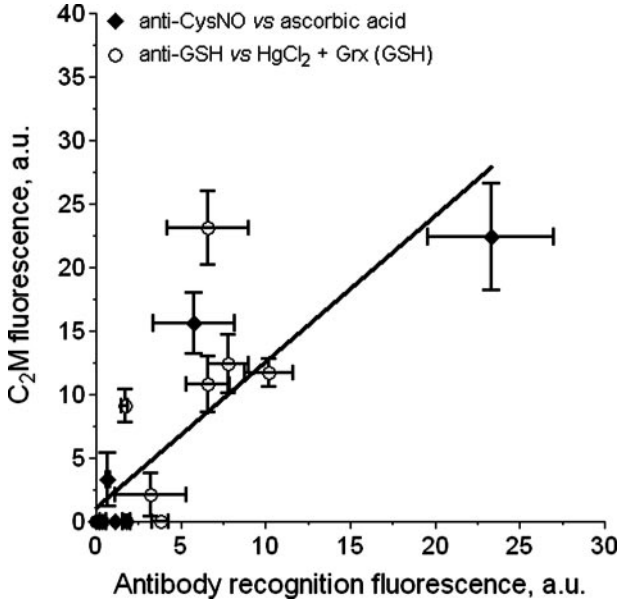

FIGURE 6. **Comparative analysis of RyR1 redox modifications screened through Western blotting and selective labeling with C_2-maleimide.** Data obtained from maleimide labeling of the ascorbate-reduced sample (shown in Fig. 2*C, left panel*) was plotted against data obtained using the anti-CysNO antibody (shown in Fig. 1*B, top panel*) and is depicted as *green circles*. Data from the maleimide labeling of the sample treated with $HgCl_2$ followed by glutaredoxin reduction (shown in Fig. 2*C, right panel*) against data obtained using the anti-GSH antibody (shown in Fig. 1*B, bottom panel*) was also plotted and is depicted as *red circles*. We next subjected all data points to a nonparametric correlation analysis (Spearman), obtaining a significant linear correlation ($r = 0.8$, $p < 0.05$). Data correspond to mean ± S.D. ($n > 2$) of the maleimide signal *versus* mean ± S.D. ($n > 6$) of the antibody recognition signal, in arbitrary units (*a.u.*). The *line* depicts data correlation, assessed by the nonparametric analysis.

(Fig. 5*A, right panel*). As seen in Fig. 5*B* (*right panel, lane E*), labeling of fragments 3 and 7 was decreased by preincubation with mercuric chloride, consistent with their *S*-nitrosylation in Fig. 5*B* (*right panel, lane B*). These findings suggest that glutaredoxin 1 reduces both *S*-nitrosylated and *S*-glutathionylated cysteines. Densitometric analysis of *S*-nitrosylated (Fig. 5*B*, *right panel, lane B*) and *S*-glutathionylated (Fig. 5*B*, *right panel, lane E*) fragments by this method is shown in Fig. 5*C*. The identity of RyR1 tryptic fragments containing specific modifications was determined with sequence-specific antibodies and/or N-terminal amino acid analysis. The fragments identified using modification-specific antibodies and those labeled under the different treatments with C_2-maleimide displayed a significant linear correlation ($r = 0.86$, $p < 0.01$ by Spearman nonparametric correlation analysis), as shown in Fig. 6. These results support the validity of this approach for identifying fragments modified by *S*-nitrosylation and *S*-glutathionylation and allow us to interpret ICAT labeling of fragments (see below) as the same selective-reduction process is used.

Identification of RyR1 Fragments Modified in Vitro by Redox Reagents—To identify RyR1 fragments that can be redox-modified *in vitro*, we treated RyR1 embedded in SR membranes with a variety of redox reagents, at *p*Ca 5 and in the absence of Mg^{2+}, as detailed under "Experimental Procedures". The redox agents used were 0.25 mM NOR-3, 0.25 mM NOC-12, 5 mM H_2O_2, 4 mM GSH plus 0.1 mM H_2O_2, or 0.25 mM GSNO. NOR-3 and NOC-12 are both NO• donors, but with very different half-lives (30 and 327 min, respectively, in PBS at 22 °C according to the manufacturer) and were used as pure *S*-nitrosylating agents. H_2O_2 (5 mM) was used as a pure oxidant (*i.e.* cross-linking agent), whereas 0.1 mM H_2O_2 in the presence of 40-fold excess GSH was employed as an *S*-glutathionylating mixture. Finally, GSNO was used to simultaneously generate *S*-nitrosylation and *S*-glutathionylation. As a control for endogenous modifications, we used RyR1 incubated only with buffer solution. All these redox agents have been shown to elicit the targeted modifications of RyR1 described in previous studies (18, 27, 29). None of the described treatments altered either the tryptic digest patterns or the sedimentation properties of the RyR1 proteolytic complex (data not shown).

Treatment with GSNO increased the *S*-nitrosylation of fragment 3 (residues 1–1509) but decreased the *S*-nitrosylation of fragments 2 and 7 (amino acid residues 3120–4475 and 3631–4475, respectively) as assessed with the anti-CysNO antibody (Fig. 7). In contrast, fragments representing residues 1–509, 1396–2401, 1509–2401, 3120–4475, and 3631–4475, all of which are also endogenously modified, were further *S*-glutathionylated (assessed with the anti-GSH antibody). In addition, fragment 1 (residues 3120–5037), which was not detected as endogenously modified, was readily *S*-glutathionylated with GSNO. Fragments representing residues 2402–2840 and 4476–5037 were not recognized by either anti-CysNO or anti-GSH antibodies.

We also compared the *S*-nitrosylation patterns obtained with different NO• donors. These data are shown in Fig. 8 and summarized in Table 2. Both NOR-3 and NOC-12 were more effective than GSNO in *S*-nitrosylating fragments 1 (residues 3120–5037), 2 (3120–4475), 3 (residues 1–1509), and 7 (3631–4475). These data suggest that cysteines in different RyR1 regions react differently, at atmospheric pO_2, with pure NO• donors than with GSNO, which can both *S*-nitrosylate and *S*-glutathionylate cysteine residues in these conditions. A similar suggestion was made by Sun *et al.* (26), who showed *S*-nitrosylation of Cys-3635 with NOC-12 but not with GSNO, which *S*-nitrosylated different cysteine residues.

As shown in Fig. 9 and summarized in Table 3, incubation with GSH plus H_2O_2 or with GSNO led to the *S*-glutathionylation of fragments 1–3 and 5–7 (amino acid residues 3120–5037, 3120–4475, 1–1509, 1396–2401, 1509–2401, and 3631–4475, respectively). One possible explanation of the ability of NOR-3 and NOC-12, but not GSNO, to *S*-nitrosylate fragments 1, 2, and 7 (all containing Cys-3635) is that *S*-glutathionylation is preferred to *S*-nitrosylation of a residue within this sequence (perhaps Cys-3635). Consistent with this proposal, GSH plus H_2O_2 abolished the endogenous *S*-nitrosylation of this region (not shown). These findings are consistent with Viner *et al.* (50), who suggested that some *S*-nitrosylated residues are more readily *S*-glutathionylated than reduced cysteine residues.

Our data can be summarized as follows (see also Tables 2 and 3). 1) RyR1 fragments 3, 5, and 6 (amino acids 1–2401) and fragments 1, 2, and 7 (covering the 3120–4475 region) are endogenously redox-modified. 2) Only these regions are susceptible to further modifications by various redox agents. 3) Only NOR-3 and NOC-12 *S*-nitrosylate fragments 2 and 7 (represent-

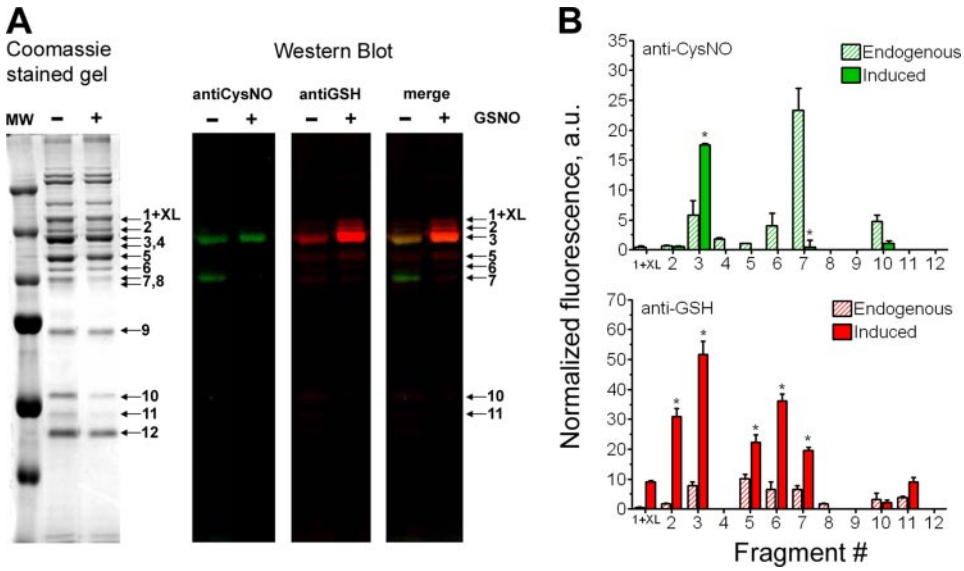

FIGURE 7. **GSNO-induced redox modifications of RyR1 in multiple sites.** SR vesicles were incubated with or without 0.25 mM GSNO and analyzed as described in Fig. 1. *A*, representative image ($n > 3$) of the CBB-stained gel (*left*) and fluorescence scan (*right*) obtained with samples incubated in the absence (*minus lanes*) or presence of GSNO (*plus lanes*); *green* and *red* signals correspond to the detection of anti-CysNO and anti-GSH, respectively, whereas a *yellow* signal indicates merging of both signals. *Numbers* on the *left* indicate molecular mass standards in kDa, and *numbers* on the *right* indicate the identity of tryptic fragments, using the numbering shown in Table 1. *1+XL* indicates the presence of fragment 1 plus a disulfide cross-link product. *B*, densitometric analysis of anti-CysNO (*green bars, top panel*) or anti-GSH (*red bars, bottom panel*) signals from images as in *A*; values correspond to mean ± S.D. ($n > 3$) of fluorescent signals normalized to CBB staining (*a.u.*, arbitrary units). * $p < 0.05$ compared with endogenous.

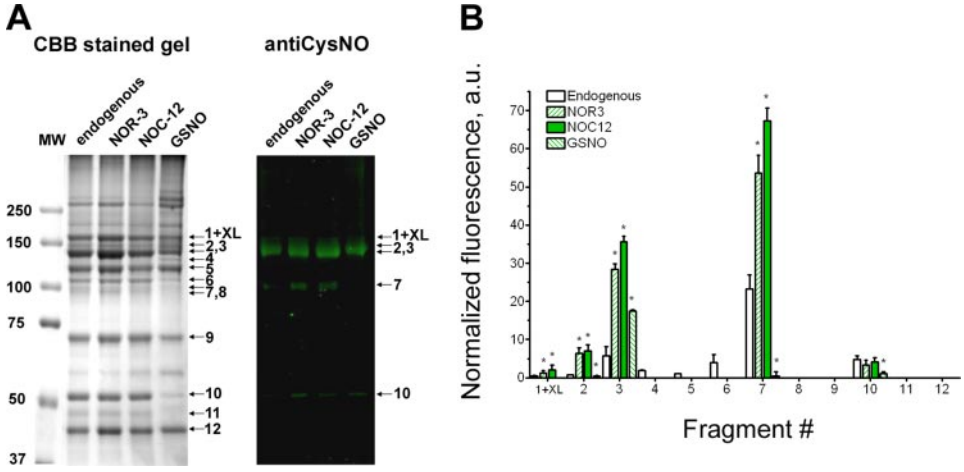

FIGURE 8. **Different NO donors elicited *S*-nitrosylation of RyR1 at different sites.** SR vesicles were incubated with 0.25 mM of either NOR-3, NOC-12, or GSNO and analyzed as described in Fig. 1. *A*, representative image ($n > 2$) of the CBB-stained gel (*left*) and fluorescence scan at 800 nm excitation wavelength (*right*). *Numbers* on the *left* indicate molecular mass standards in kDa, and *numbers* on the *right* indicate the identity of tryptic fragments, using the numbering shown in Table 1. *1+XL* indicates the presence of fragment 1 plus a disulfide cross-link product. *B,* densitometric analysis of anti-CysNO signals from images as in *A*; values correspond to mean ± S.D. ($n > 2$) of fluorescent signals normalized to CBB staining (*a.u.*, arbitrary units). * $p < 0.05$ compared with endogenous.

ing the 3120–4475 region). 4) Exposure to *S*-glutathionylating agents overrides the endogenous *S*-nitrosylation of region 3120–4475.

Functional Effect of Incubating SR Vesicles with Redox Reagents on RyR1 Activity—As widely reported, ryanodine binds to RyR1 only when the channel is in the open conformation. Thus, we set on analyzing the effect of *S*-nitrosylation or *S*-glutathionylation on the apparent affinity of RyR1 for radiolabeled ryanodine in equilibrium binding studies, as detailed under "Experimental Procedures." As shown in Table 4, the apparent K_d value of the channel for [^{3}H]ryanodine binding is significantly increased following incubation of SR vesicles with either NOR-3 or the mixture of GSH and H_2O_2. These data show that redox modifications of RyR1 increase the open probability of the channel and are in agreement with our previous study (18).

Identification of the RyR1 Cysteine Residues Modified by Redox Reagents—Using a similar redox switch approach to that described above, we used ICAT technology to identify *S*-nitrosylated, *S*-glutathionylated, and oxidized cysteine residues (Fig. 10). The ICAT®-cleavable molecules (see Fig. 10*A*) are sulfhydryl-reactive probes with biotin tags and are supplied as light or heavy isotopes (mass difference of 9 atomic mass units because of the presence of 9 × ^{13}C atoms in the heavy isotope). The biotin tag is used to selectively purify the ICAT-labeled fragments using avidin-affinity chromatography. This approach significantly increases the signal to noise ratio for mass spectrometry detection of peptides following complete tryptic digestion (see diagram in Fig. 10*B*).

Following selective reduction of cysteines of RyR1 tryptic fragments, the samples were ICAT-labeled and subjected to limited digestion with trypsin. After purification of labeled fragments, the biotin tag was cleaved, and peptides were analyzed by MALDI-TOF spectrometry by two separate and independent laboratories (see "Experimental Procedures"). Fig. 10*C* illustrates an example of a whole MALDI-TOF spectrum obtained by this method. This particular spectrum shows the ICAT-labeled peptides obtained from an endogenously modified sample reduced with glutaredoxin. The following criteria were applied for identification of the ICAT-labeled peptides. 1) There must be two peaks separated by 9.03 ± 0.03 atomic mass units. 2) The intensity of these peaks must be at least 2-fold above the background signal. 3) The ratio of intensity of these peaks must be 1 ± 0.3. Fig. 10*D* shows an example of a peak pair fulfilling these criteria, obtained from a section of the spectrum shown in Fig. 10*C*. Peaks that did not meet the above three criteria were disregarded.

Upon identification of the ICAT peptide peaks, the mass of the heavy or light ICAT was subtracted from the peaks, and the data were analyzed using Mascot Tool (Matrix Science server). Ten out of 13 peak pairs in the spectrum were identified as RyR1. An additional peak pair was found to correspond to free ICAT molecules, appearing at 1022 and 1031 *m*/*z* (confirmed by the manufacturer). Other peak pairs represented peptides from proteins known to be minor contaminants in the RyR1 preparation (*e.g.* sarcoplasmic/endoplasmic Ca^{2+}-ATPase, type 1).

Two additional fingerprinting analyses were performed using the P11716 accession number for the rabbit RyR1 sequence. The first analysis was performed with light and heavy peptide mass data, using the FindPept Tool (ExPASy Proteomics server) customizing the ICAT modifications as $C_{10}H_{17}O_3N_3$ and $C_{10}H_{26}O_3N_3$ (light and heavy ICAT; note the change in H atom number to account for the 9 atomic mass units and mass difference). Thirteen pairs of peaks were detected, and again 10 corresponded to RyR1-specific ICAT-labeled peptides (summarized in Table 5), in complete agreement with the Mascot data.

TABLE 2

RyR1 regions with endogenous and induced *S*-nitrosylation

SR vesicles were treated with or without 0.25 mM of either NO• donor as described under "Experimental Procedures." Following limited proteolysis and isolation of the RyR1, major tryptic complex samples were subjected to nonreducing Laemmli SDS-PAGE and Western blotting with an anti-CysNO antibody as detailed under "Experimental Procedures." Table shows the summary of the antibody recognition data shown in Fig. 6. Numbering is as shown in Table I. Only fragments that displayed detectable modifications are shown. 1+XL indicates the presence of fragment 1 plus a disulfide cross-linked product with the same molecular mass as this fragment. The + signs indicate qualitative detection of the fluorescent signal as follows: +, low intensity; ++, intermediate intensity; +++, high intensity.

Fragment	Endogenous	NOR-3	NOC-12	GSNO
1+XL	Not detected	++	++	Not detected
2	+	+	+	Not detected
3	+	+++	+++	++
7	+	+++	+++	Not detected
10	+	++	++	+

The second fingerprinting analysis consisted of the identification of all possible cysteine-containing tryptic peptides from RyR1 (list obtained with the PeptideCutter tool from the ExPASy server), with the addition of 227.13 and 226.16 atomic mass units to the mass of each peptide. These values were then used to manually search for peak pairs. For instance, in the spectrum displayed in Fig. 10*C*, no additional peak pairs corresponding to RyR1 peptides were found, strongly supporting the previous assignments. We found that Cys-36, Cys-315, Cys-811, Cys-906, Cys-1591, Cys-2326, Cys-2363, Cys-3193, and Cys-3635 were endogenously modified (either *S*-nitrosylated or *S*-glutathionylated because the reduction was with glutaredoxin).

By using the above approach together with the redox switch reductions, we identified cysteine residues that are modified *in vitro*. Our results are summarized in Table 5. Incubation with GSNO led to *S*-nitrosylation of Cys-253, Cys-315, Cys-811, Cys-906, Cys-1040, and Cys-1303 and *S*-glutathionylation of Cys-36, Cys-811, Cys-906, Cys-1591, Cys-2326, Cys-2363, Cys-3193, and Cys-3635. NOR-3 promoted *S*-nitrosylation of Cys-253, Cys-315, Cys-811, Cys-906, Cys-1040, Cys-1303, and Cys-3635, whereas GSH plus H_2O_2 caused *S*-glutathionylation of Cys-36, Cys-253, Cys-315, Cys-811, Cys-906, Cys-1591, Cys-2326, Cys-2363, Cys-3193, and Cys-3635.

Cysteine residues on RyR1 also undergo oxidation-induced disulfide formation (27). To identify cysteines involved in disulfide formation, we treated SR vesicles with 5 mM H_2O_2 (in the absence of GSH) and isolated RyR1 as a proteolytic complex after trypsin digestion. Following reduction with glutaredoxin to remove any endogenous *S*-nitrosylation or *S*-glutathionylation, we irreversibly blocked all reduced cysteine residues with NEM. The samples were acetone-precipitated to remove excess NEM and reduced with DTT to cleave disulfide cross-links. After removal of the reducing agent, the RyR1 tryptic fragments were ICAT-labeled and analyzed by mass spectrometry. We identified cysteine residues 36, 2326, 2363, and 3635 as disulfide cross-linked residues by H_2O_2 (Table 6).

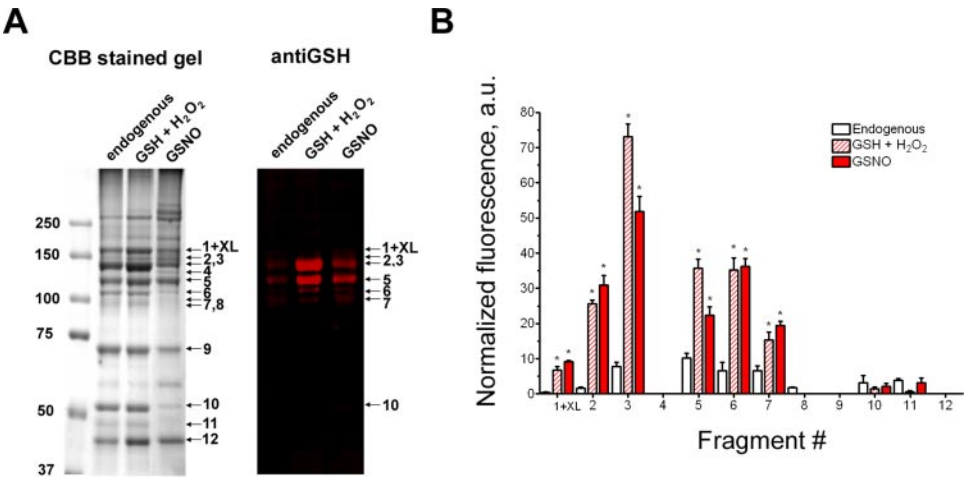

FIGURE 9. **Different *S*-glutathionylating agents modified of RyR1 at the same sites.** SR vesicles were incubated with either 4 mM GSH plus 0.1 mM H_2O_2 or 0.25 mM GSNO and analyzed as in Fig. 1. *A*, representative image ($n > 2$) of the CBB-stained gel (*left*) and fluorescence scan at 700 nm excitation wavelength (*right*). *Numbers* on the *left* indicate molecular mass standards in kDa, and *numbers* on the *right* indicate the identity of tryptic fragments, using the numbering shown in Table 1. *1+XL* indicates the presence of fragment 1 plus a disulfide cross-link product. *B*, densitometric analysis of anti-GSH signals from images as in *A*; values correspond to mean ± S.D. ($n > 2$) of fluorescent signals normalized to CBB staining (*a.u.*, arbitrary units). * $p < 0.05$ compared with endogenous.

DISCUSSION

Reactive oxygen species and nitric oxide (NO•) derivatives are continually synthesized by skeletal muscle and are endogenous modulators of muscle function. These redox-active molecules exert tonic influences on a variety of processes within the myocyte, including EC coupling (51). The sarcoplasmic reticulum Ca^{2+}-release channel (RyR1) is one of the major redox targets in skeletal muscle (21–23, 52).

Hyper-reactive sulfhydryl groups associated with RyR1 have a well defined redox potential that is sensitive to the cellular environment (14, 53). Feng *et al.* (14) suggested that channel activators decrease the redox potential leading to modification of

TABLE 3

RyR1 regions with endogenous and induced *S*-glutathionylation

SR vesicles were treated with or without the mixture of 4 mM GSH plus 0.1 mM H_2O_2 or 0.25 mM GSNO as described under "Experimental Procedures." Following limited proteolysis and isolation of the RyR1 major tryptic complex, samples were subjected to nonreducing Laemmli SDS-PAGE and Western blotting with an anti-GSH antibody as detailed under "Experimental Procedures." Table shows the summary of the antibody recognition data shown in Fig. 7. Numbering is as shown in Table 1. Only fragments that displayed detectable modifications are shown. *1+XL* indicates the presence of fragment 1 plus a disulfide cross-linked product with the same molecular mass as this fragment. The + signs indicate qualitative detection of the fluorescent signal as follows: +, low intensity; ++, intermediate intensity; +++, high intensity.

Fragment	Endogenous	GSH + H_2O_2	GSNO
1+XL	Not detected	+++	+++
2	+	+++	+++
3	++	+++	++
5	+	+++	++
6	++	+++	+++
7	+	++	++
10	+	++	++
11	+	Not detected	+

TABLE 4

Effect of RyR1 redox modifications on ryanodine binding

SR vesicles were treated with or without 0.25 mM NOR-3 or the mixture of 4 mM GSH plus 0.1 mM H_2O_2 as described under "Experimental Procedures." Following washing of redox agents, equilibrium ryanodine binding was performed in the presence of 0.2 mM Ca^{2+}, as detailed under "Experimental Procedures." K_d values were calculated from nonlinear regression analysis of respective saturation curves; these values were in agreement with those calculated from Scatchard plots. Values represent the mean of at least three independent determinations ± S.D. **, $p < 0.01$ compared with control.

Treatment	K_d
	nM
Buffer solution (Control)	7.5 ± 1.1
0.25 mM NOR-3	3.3 ± 1.2**
4 mM GSH plus 0.1 mM H_2O_2	4.1 ± 0.6**

cysteine residues and channel opening, whereas inhibitors increase the redox potential leading to the reduction of disulfides and channel closing. These hyper-reactive cysteines on RyR1 are thought to be targets for disulfide cross-linking, *S*-nitrosylation, and/or *S*-glutathionylation. All three modifications increase channel activity but appear to do so by different mechanisms. Both *S*-nitrosylation and oxidation increase the sensitivity of the channel to Ca^{2+} activation, whereas *S*-glutathionylation decreases selectively the sensitivity of the channel to inhibition by Mg^{2+} (18).

One redox-sensitive cysteine (Cys-3635) has been proposed to play a major role in redox modulation of RyR1. We find that Cys-3635 is likely to play a modulatory role in voltage-gated EC coupling (Fig. 1), in addition to its role in regulating the interaction of calmodulin with the channel (30, 32) and the response of the channel to nitrosylating agents at low pO_2 (33). Yet our data also suggest that Cys-3635 is not required for the enhancement of RyR1 activity caused by H_2O_2 (Fig. 2).

Voss *et al.* (35) identified a number of RyR1 cysteines that were hyper-reactive to the fluorescent maleimide, CPM, in the presence of 10 mM Mg^{2+}. These labeled cysteines included Cys-1040, Cys-1303, Cys-2436, Cys-2565, Cys-2606, Cys-2611, and Cys-3635. We now identify nine different cysteines in RyR1 that are endogenously modified: Cys-36, Cys-315, Cys-811, Cys-906, Cys-1591, Cys-2326, Cys-2363, Cys-3193, and Cys-3635. This subset of cysteines plus Cys-253, Cys-1040, and Cys-1303 can also be modified, after addition of redox reagents *in vitro*, by *S*-nitrosylation, *S*-glutathionylation, or oxidation to disulfides (at *p*Ca 5 and in the absence of Mg^{2+}). Only three of these residues correspond to cysteines that are hyper-reactive with CPM (35). The finding of different modified cysteines in the two studies may reflect intrinsic differences in the modifying reagents employed or may arise from the different labeling conditions used. Liu *et al.* (5) have shown that RyR1 is *S*-alkylated by CPM only in the presence of 10 mM Mg^{2+}, a condition rendering a significant population of channels in the closed state. We chose to label under conditions that, depending on the redox agent used, alter either the Ca^{2+} or the Mg^{2+} sensitivity of RyR1, as we have shown previously (18). Although at *p*Ca 5 and in the absence of Mg^{2+} a significant fraction of the channel population is likely to be in the open state (20), more studies are needed to address whether RyR1 cysteine sensitivity to the modifications analyzed here correlates with the functional states of the channel. In our study, *S*- nitrosylation, *S*-glutathionylation, and oxidation modified many of the same residues, but we found that several cysteines undergo selective redox modifica-

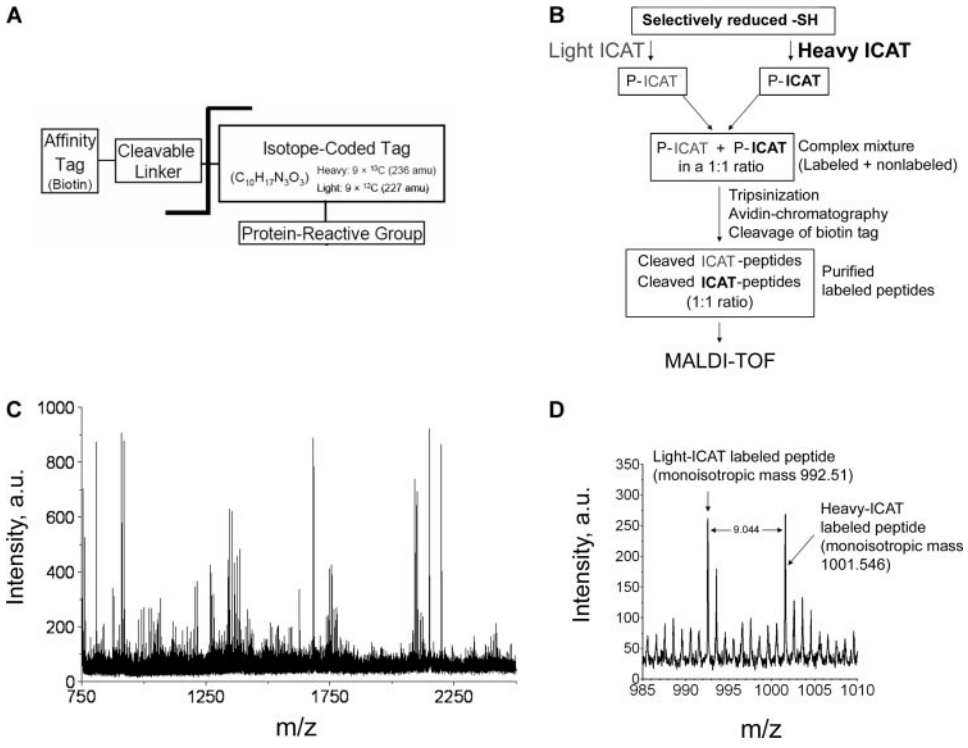

FIGURE 10. **MALDI-TOF spectrum of ICAT-labeled RyR1 with endogenous redox modifications.** *A*, structure of the ICAT reagent, as provided by the manufacturer (Applied Biosystems). *B*, diagram of ICAT labeling (see "Experimental Procedures" for details). *C*, endogenously/spontaneously modified RyR1 tryptic fragments were selectively reduced with glutaredoxin and ICAT-labeled as detailed under "Experimental Procedures." Following ICAT-labeled peptides purification, the sample was analyzed by MALDI-TOF; a representative spectrum is shown. *D*, typical ICAT-peptide signal obtained from the spectrum shown in *C*.

TABLE 5

Representative mass fingerprinting analysis of RyR1 ICAT-labeled peptides

SR vesicles bearing endogenous redox modifications were subjected to limited proteolysis and isolation of the RyR1 major tryptic complex samples as detailed under "Experimental Procedures." Following selective reduction with glutaredoxin, fragments were ICAT-labeled and subjected to exhaustive trypsinization. After avidin-affinity chromatography and cleavage of the biotin tag, samples were analyzed by MALDI-TOF spectrometry, as described under "Experimental Procedures." Pairs of heavy-light ICAT peptides were identified following specific criteria (detailed in the text), and mass fingerprinting analysis was performed. The table summarizes the findings of 10 signals out of 13 ICAT-labeled peptides found, using the FindPept Tool (see details in the text).

Light ICAT (*m/z*)	Heavy ICAT (*m/z*)	Differentiation (*m/z*)	Start residue	End residue	Sequence	Cys
992.557	1001.575	9.005	3631	3637	(R)AVVA**C**FR(M)	3635
1058.523	1067.558	9.035	311	317	(K)ATSF**C**FR(V)	315
1206.623	1215.640	9.017	1586	1594	(K)NPAPQ**C**PPR(L)	1591
1344.726	1353.745	9.019	2360	2369	(R)KPE**C**FGPALR(G)	2363
1377.712	1386.735	9.023	35	45	(K)L**C**LAAEGFGNR(L)	36
1425.803	1434.773	8.970	3186	3196	(K)LRPALGE**C**LAR(L)	3193
1747.794	1756.819	9.025	2317	2330	(K)GYPDIGWNP**C**GGER(Y)	2326
2091.088	2100.106	9.018	802	818	(K)FLPPPGYAP**C**HEAVLPR(E)	811
2115.084	2124.102	9.018	903	918	(R)LHP**C**LVNFHSLPEPER(N)	906
2411.302	2420.347	9.045	311	329	(K)ATSF**C**FRVSKEKLDTAPKR(D)	315

TABLE 6

RyR1 cysteine residues displaying endogenous or induced redox modifications

SR vesicles treated with or without various redox agents were subjected to limited proteolysis and isolation of the RyR1 major tryptic complex samples as detailed under "Experimental Procedures." Following selective reduction, fragments were ICAT-labeled and subjected to exhaustive trypsinization. After avidin-affinity chromatography and cleavage of the biotin tag, samples were analyzed through MALDI-TOF spectrometry, as described under "Experimental Procedures." The table summarizes the cysteine residues identified by mass fingerprinting analysis, as detailed in the text. 1+XL indicates the presence of fragment 1 plus a disulfide cross-linked product with the same molecular mass as this fragment.

Cys	Fragment (antibody recognition)	Endogenous	Oxidation	*S*-Nitrosylation		*S*-Glutathionylation	
				NOR-3	GSNO	GSH + H_2O_2	GSNO
36	3	+	+			+	+
253	(anti-CysNO			+	+	+	
315	and anti-GSH)	+		+	+	+	
811	3 and 8	+		+	+	+	+
906	(anti-CysNO	+		+	+	+	+
1040	and anti-GSH)[a]			+	+		
1303				+	+		
1591	5 and 6	+				+	+
2326	(anti-GSH only)	+	+			+	+
2363		+	+			+	+
3193	1+XL and 2 (anti-CysNO and anti-GSH)	+				+	+
3635	1+XL, 2, and 7 (anti-CysNO and anti-GSH)	+	+	+		+	+

[a] This is only in the case of fragment 3.

tions. Cys-253, Cys-315, Cys-811, Cys-906, and Cys-3635 can be either *S*-glutathionylated or *S*-nitrosylated. Cys-1040 and Cys-1303 appear to be exclusively *S*-nitrosylated, whereas Cys-1591 and Cys-3193 are exclusively *S*-glutathionylated. All cysteines that can be oxidized to disulfides (Cys-36, Cys-2326, Cys-2363, and Cys-3635) can also be *S*-glutathionylated, but only Cys-3635 can also be *S*-nitrosylated. These differences in the targets of modifications as well as the differences in the modifications themselves may help explain how different modifications produce different outcomes.

We also found that different NO$^{\bullet}$ donors can *S*-nitrosylate different cysteines. NOR-3 and NOC-12, but not GSNO, *S*-nitrosylate Cys-3635 (consistent with the findings of Sun *et al.* (26)). GSNO, however, can promote both *S*-nitrosylation and *S*-glutathionylation of the channel (29). Because Cys-3635 can also be *S*-glutathionylated, it is possible that competition between *S*-glutathionylation and *S*-nitrosylation prevents the *S*-nitrosylation of Cys-3635 by GSNO. The relative contributions of these two modifications of Cys-3635 to alterations in RyR1 activity have not been established.

The redox-modified cysteines that we identify in this study are scattered throughout the cytoplasmic domain of RyR1. Residues Cys-315, Cys-811, Cys-906, Cys-1040, and Cys-1303 are within an N-terminal region of RyRs that has been suggested to form part of the FKBP12-binding site (54), whereas residues Cys-2326, Cys-2363, and Cys-3635 are located close to both the calmodulin- (31, 33, 55–57) and FKBP12-binding sites (58). The location of these redox-sensitive cysteine residues in regions known to interact with calmodulin and FKBP12 may help to explain previous results showing that different redox modifications of RyR1 differentially alter binding of these accessory proteins (29, 33, 59). In addition, some of the redox-reactive cysteine residues identified in the present study are located within the mutation clusters associated with malignant hyperthermia. Residues Cys-36, Cys-253 and Cys-315 are located in the mutation region 1 (corresponding to amino acids 36–615 in the rabbit sequence), whereas residues Cys-2326 and Cys-2363 are located in the mutation region 2 (corresponding to amino acids 2117–2458 in the rabbit sequence) (3). Naturally occurring mutations in these clusters have been shown to alter RyR1 response to modulators (see Refs. 58 and 60–67; for reviews see Loke and MacLennan (68) and Robinson *et al.* (69)). These cysteine residues may have a role in regulating RyR1 modulators access to or affinity for the channel, presumably explaining the changes observed in the channel response to modulators upon redox modifications (21–23, 52).

We have identified four cysteines that form disulfide bonds in RyR1 as follows: Cys-36, Cys-2326, Cys-2363, and Cys-3635.

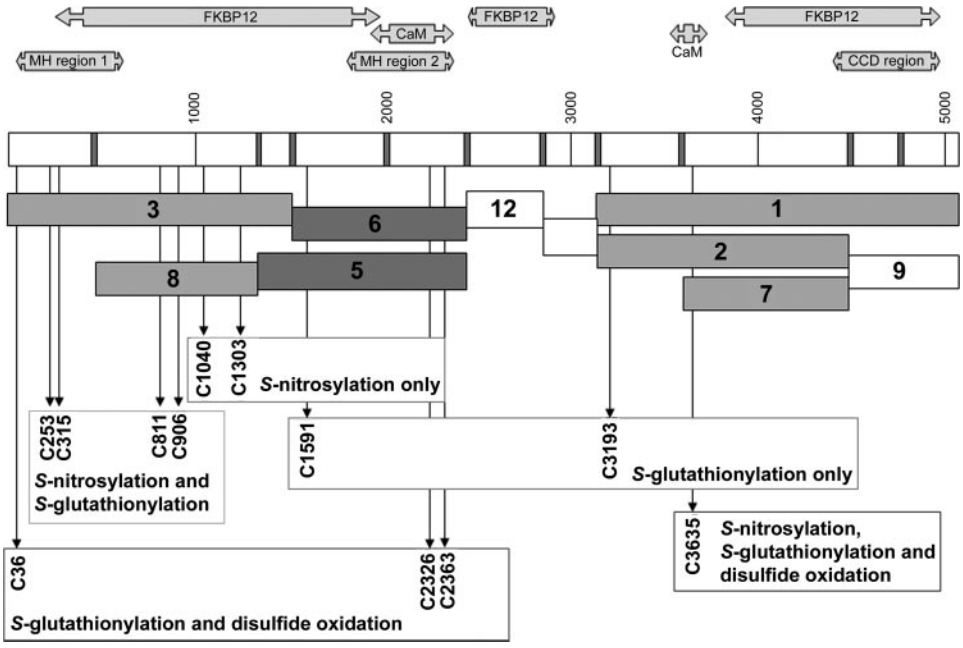

FIGURE 11. **Map of redox modifications of RyR1.** Schematic of RyR1 amino acid sequence with the tryptic cleavage sites shown in *gray*. Above this sequence are depicted the mutation clusters associated with malignant hyperthermia (*MH*) and central core disease (*CCD*) (3, 68), and the calmodulin (*CaM*) and FKBP12-binding regions (according to Refs. 31 and 54–67). The map of fragments obtained in this study is shown below the RyR1 sequence, and numbering of fragments is the same as in Table 1. Tryptic fragments susceptible to both *S*-nitrosylation and *S*-glutathionylation are shown in light gray; those susceptible only to *S*-glutathionylation are shown in dark gray. Cysteine residues identified by mass spectrometry are grouped according to their susceptibility to *in vitro* modification.

Abramson and Salama (70) have suggested that the formation of a disulfide bond in response to oxidants drives a conformational change in RyR1 that promotes its opening. One candidate for this mechanism is the disulfide bond between Cys-4958 and Cys-4961. Hurne *et al.* (71) mutated these cysteines of the C-terminal tail of RyR1 and found that the channel failed to respond to activators and did not support skeletal EC coupling. In our study neither one of these cysteines were identified as forming disulfide bonds in response to H_2O_2, possibly suggesting that either this putative disulfide bond is very labile or is not formed in our conditions. A second candidate disulfide is more consistent with our current findings. Moore *et al.* (30) demonstrated that Cys-3635 forms a disulfide bond with a neighboring subunit and in doing so limits the access of calmodulin to its binding site (32). Because Ca^{2+}-calmodulin is an inhibitor of the channel, the net result would be increased activity of the channel at high Ca^{2+} concentrations. We suggest that Cys-36, Cys-2326, or Cys-2363 is likely to be the partner cysteine in the disulfide bond with Cys-3635, with the two remaining cysteines forming a second disulfide. The partner of Cys-3635 in this disulfide bond remains to be identified. In light of our functional studies, this disulfide bond is likely to have a discrete role in EC coupling as the C3635A mutation decreases the voltage sensitivity of RyR1-mediated Ca^{2+} release (orthograde coupling). Cys-3635 appears not to be required in the redox sensor of the channel, because its mutant ion does not change the ability of the channel to be activated by H_2O_2. On the other hand, all four of the cysteines identified as disulfide forming can also be *S*-glutathionylated, but only Cys-3635 can be *S*-nitrosylated. Cys-3635 is also a hyper-reactive target for *S*-alkylation by NEM (30) and CPM (35), suggesting that Cys-3635 is one of the most hyper-reactive cysteine residues in the RyR1 molecule. Yet Cys-3635 appears not to be required for the redox sensor function of the channel, because the C3635A mutation does not modify the significant activation of the channel by H_2O_2. These findings strongly suggest that the channel redox sensor is comprised not just of a single residue but by multiple cysteine residues. Accordingly, the study of the individual contributions of each cysteine becomes a very complex endeavor. Further selective mutational analysis is part of a long term effort to understand the relevance of each of the identified redox-sensitive cysteine residues in modifying RyR1 channel function.

In summary (see Fig. 11), we show that 12 of the 100 cysteines on RyR1 can be redox-modified and that 9 of these cysteines appear to be endogenously modified to some extent. We also show that the different redox agents target some of the same cysteines, but Cys-1040 and Cys-1303 are exclusively *S*-nitrosylated, whereas Cys-1591 and Cys-3193 are exclusively *S*-glutathionylated. On the other hand, Cys-3635 can be *S*-nitrosylated, *S*-glutathionylated, or oxidized to form a disulfide and also influences Ca^{2+} release during EC coupling.

The study of protein redox modifications is becoming a novel field in research. These modifications are extremely difficult to study because they are reversible by reducing agents commonly used in protein biochemistry. They are also destroyed by the ionization procedure involved in mass spectrometry analyses. To our knowledge, this study represents the first work describing a high throughput technology that allows the differential mapping of disulfide-oxidized, *S*-nitrosylated, and *S*-glutathionylated cysteines by mass spectrometry.

Acknowledgments—We thank Dr. Robert Cook for help with ICAT labeling and initial mass spectrometry studies and Dr. Pumin Zhang for help in designing plasmid construction strategy and the pML104/DH10β strain. We also thank Dr. David MacLennan for the pMT2 vector containing the full-length RyR1 cDNA, Dr. Paul Allen for the access to dyspedic mice, and Dr. Andrew Marks for the rabbit polyclonal anti-RyR1 directed against the sequence 5029–5037. We acknowledge the technical assistance of Rong He in the plasmid construction of wild-type and C3635A mutant of RyR1.

REFERENCES

1. Fill, M., and Copello, J. A. (2002) *Physiol. Rev.* **82,** 893–922
2. Meissner, G. (2002) *Front. Biosci.* **7,** D2072–D2080
3. Hamilton, S. L. (2005) *Cell Calcium* **38,** 253–260
4. Takeshima, H., Nishimura, S., Matsumoto, T., Ishida, H., Kangawa, K., Minamino, N., Matsuo, H., Ueda, M., Hanaoka, M., Hirose, T., and Numa,

S. (1989) *Nature* **339,** 439–445
5. Liu, G., Abramson, J. J., Zable, A. C., and Pessah, I. N. (1994) *Mol. Pharmacol.* **45,** 189–200
6. Stoyanovsky, D. A., Salama, G., and Kagan, V. E. (1994) *Arch. Biochem. Biophys.* **308,** 214–221
7. Favero, T. G., Zable, A. C., and Abramson, J. J. (1995) *J. Biol. Chem.* **270,** 25557–25563
8. Aghdasi, B., Reid, M. B., and Hamilton, S. L. (1997) *J. Biol. Chem.* **272,** 25462–25467
9. Stoyanovsky, D., Murphy, T., Anno, P. R., Kim, Y. M., and Salama, G. (1997) *Cell Calcium* **21,** 19–29
10. Zable, A. C., Favero, T. G., and Abramson, J. J. (1997) *J. Biol. Chem.* **272,** 7069–7077
11. Suzuki, Y. J., Cleemann, L., Abernethy, D. R., and Morad, M. (1998) *Free Radic. Biol. Med.* **24,** 318–325
12. Suko, J., Drobny, H., and Hellmann, G. (1999) *Biochim. Biophys. Acta* **1451,** 271–287
13. Eu, J. P., Sun, J., Xu, L., Stamler, J. S., and Meissner, G. (2000) *Cell* **102,** 499–509
14. Feng, W., Liu, G., Allen, P. D., and Pessah, I. N. (2000) *J. Biol. Chem.* **275,** 35902–35907
15. Sun, J., Xu, L., Eu, J. P., Stamler, J. S., and Meissner, G. (2001) *J. Biol. Chem.* **276,** 15625–15630
16. Oba, T., Murayama, T., and Ogawa, Y. (2002) *Am. J. Physiol.* **282,** C684–C692
17. Xia, R., Webb, J. A., Gnall, L. L., Cutler, K., and Abramson, J. J. (2003) *Am. J. Physiol.* **285,** C215–C221
18. Aracena, P., Sanchez, G., Donoso, P., Hamilton, S. L., and Hidalgo, C. (2003) *J. Biol. Chem.* **278,** 42927–42935
19. Cheong, E., Tumbev, V., Abramson, J., Salama, G., and Stoyanovsky, D. A. (2005) *Cell Calcium* **37,** 87–96
20. Marengo, J. J., Hidalgo, C., and Bull, R. (1998) *Biophys. J.* **74,** 1263–1277
21. Eu, J. P., Xu, L., Stamler, J. S., and Meissner, G. (1999) *Biochem. Pharmacol.* **57,** 1079–1084
22. Hidalgo, C., Donoso, P., and Carrasco, M. A. (2005) *IUBMB Life* **57,** 315–322
23. Hamilton, S. L., and Reid, M. B. (2000) *Antioxid. Redox. Signal.* **2,** 41–45
24. Pessah, I. N., and Feng, W. (2000) *Antioxid. Redox. Signal.* **2,** 17–25
25. Salama, G., Menshikova, E. V., and Abramson, J. J. (2000) *Antioxid. Redox. Signal.* **2,** 5–16
26. Sun, J., Xu, L., Eu, J. P., Stamler, J. S., and Meissner, G. (2003) *J. Biol. Chem.* **278,** 8184–8189
27. Aghdasi, B., Zhang, J. Z., Wu, Y., Reid, M. B., and Hamilton, S. L. (1997) *J. Biol. Chem.* **272,** 3739–3748
28. Wu, Y., Aghdasi, B., Dou, S. J., Zhang, J. Z., Liu, S. Q., and Hamilton, S. L. (1997) *J. Biol. Chem.* **272,** 25051–25061
29. Aracena, P., Tang, W., Hamilton, S. L., and Hidalgo, C. (2005) *Antioxid. Redox. Signal.* **7,** 870–881
30. Moore, C. P., Zhang, J. Z., and Hamilton, S. L. (1999) *J. Biol. Chem.* **274,** 36831–36834
31. Moore, C. P., Rodney, G., Zhang, J. Z., Santacruz-Toloza, L., Strasburg, G., and Hamilton, S. L. (1999) *Biochemistry* **38,** 8532–8537
32. Zhang, H., Zhang, J. Z., Danila, C. I., and Hamilton, S. L. (2003) *J. Biol. Chem.* **278,** 8348–8355
33. Sun, J., Xin, C., Eu, J. P., Stamler, J. S., and Meissner, G. (2001) *Proc. Natl. Acad. Sci. U. S. A.* **98,** 11158–11162
34. Cheong, E., Tumbev, V., Stoyanovsky, D., and Salama, G. (2005) *Cell Calcium* **38,** 481–488
35. Voss, A. A., Lango, J., Ernst-Russell, M., Morin, D., and Pessah, I. N. (2004) *J. Biol. Chem.* **279,** 34514–34520
36. Callaway, C., Seryshev, A., Wang, J. P., Slavik, K. J., Needleman, D. H., Cantu, C., 3rd, Wu, Y., Jayaraman, T., Marks, A. R., and Hamilton, S. L. (1994) *J. Biol. Chem.* **269,** 15876–15884
37. Hamilton, S. L., Alvarez, R. M., Fill, M., Hawkes, M. J., Brush, K. L., Schilling, W. P., and Stefani, E. (1989) *Anal. Biochem.* **183,** 31–41
38. Lowry, O. H., Rosebrough, N. J., Farr, A. L., and Randall, R. J. (1951) *J. Biol. Chem.* **193,** 265–275
39. Chelu, M. G., Goonasekera, S. A., Durham, W. J., Tang, W., Lueck, J. D., Riehl, J., Pessah, I. N., Zhang, P., Bhattacharjee, M. B., Dirksen, R. T., and Hamilton, S. L. (2006) *FASEB J.* **20,** 329–330
40. Laemmli, U. K. (1970) *Nature* **227,** 680–685
41. Nakai, J., Dirksen, R. T., Nguyen, H. T., Pessah, I. N., Beam, K. G., and Allen, P. D. (1996) *Nature* **380,** 72–75
42. Chu, A., Diaz-Munoz, M., Hawkes, M. J., Brush, K., and Hamilton, S. L. (1990) *Mol. Pharmacol.* **37,** 735–741
43. Jaffrey, S. R., and Snyder, S. H. (2001) *Sci. STKE 2001,* PL1
44. Lind, C., Gerdes, R., Hamnell, Y., Schuppe-Koistinen, I., von Lowenhielm, H. B., Holmgren, A., and Cotgreave, I. A. (2002) *Arch. Biochem. Biophys.* **406,** 229–240
45. Ewing, J. F., and Janero, D. R. (1998) *Free Radic. Biol. Med.* **25,** 621–628
46. Shelton, M. D., Chock, P. B., and Mieyal, J. J. (2005) *Antioxid. Redox. Signal.* **7,** 348–366
47. Kahlos, K., Zhang, J., Block, E. R., and Patel, J. M. (2003) *Mol. Cell. Biochem.* **254,** 47–54
48. Huber, S. C., and Hardin, S. C. (2004) *Curr. Opin. Plant Biol.* **7,** 318–322
49. Fernandes, A. P., and Holmgren, A. (2004) *Antioxid. Redox. Signal.* **6,** 63–74
50. Viner, R. I., Williams, T. D., and Schoneich, C. (1999) *Biochemistry* **38,** 12408–12415
51. Jackson, M. J. (2005) *Philos. Trans. R. Soc. Lond. B Biol. Sci.* **360,** 2285–2291
52. Pessah, I. N., Kim, K. H., and Feng, W. (2002) *Front. Biosci.* **7,** A72–A79
53. Feng, W., and Pessah, I. N. (2002) *Methods Enzymol.* **353,** 240–253
54. Masumiya, H., Wang, R., Zhang, J., Xiao, B., and Chen, S. R. (2003) *J. Biol. Chem.* **278,** 3786–3792
55. Yamaguchi, N., Xin, C., and Meissner, G. (2001) *J. Biol. Chem.* **276,** 22579–22585
56. Rodney, G. G., Moore, C. P., Williams, B. Y., Zhang, J. Z., Krol, J., Pedersen, S. E., and Hamilton, S. L. (2001) *J. Biol. Chem.* **276,** 2069–2074
57. Rodney, G. G., Krol, J., Williams, B., Beckingham, K., and Hamilton, S. L. (2001) *Biochemistry* **40,** 12430–12435
58. Gaburjakova, M., Gaburjakova, J., Reiken, S., Huang, F., Marx, S. O., Rosemblit, N., and Marks, A. R. (2001) *J. Biol. Chem.* **276,** 16931–16935
59. Zhang, J. Z., Wu, Y., Williams, B. Y., Rodney, G., Mandel, F., Strasburg, G. M., and Hamilton, S. L. (1999) *Am. J. Physiol.* **276,** C46–C53
60. Zorzato, F., Scutari, E., Tegazzin, V., Clementi, E., and Treves, S. (1993) *Mol. Pharmacol.* **44,** 1192–1201
61. Chen, S. R., and MacLennan, D. H. (1994) *J. Biol. Chem.* **269,** 22698–22704
62. Richter, M., Schleithoff, L., Deufel, T., Lehmann-Horn, F., and Herrmann-Frank, A. (1997) *J. Biol. Chem.* **272,** 5256–5260
63. Tong, J., Oyamada, H., Demaurex, N., Grinstein, S., McCarthy, T. V., and MacLennan, D. H. (1997) *J. Biol. Chem.* **272,** 26332–26339
64. Tong, J., McCarthy, T. V., and MacLennan, D. H. (1999) *J. Biol. Chem.* **274,** 693–702
65. Du, G. G., Oyamada, H., Khanna, V. K., and MacLennan, D. H. (2001) *Biochem. J.* **360,** 97–105
66. Bultynck, G., De Smet, P., Rossi, D., Callewaert, G., Missiaen, L., Sorrentino, V., De Smedt, H., and Parys, J. B. (2001) *Biochem. J.* **354,** 413–422
67. George, C. H., Yin, C. C., and Lai, F. A. (2005) *Cell Biochem. Biophys.* **42,** 197–222
68. Loke, J., and MacLennan, D. H. (1998) *Am. J. Med.* **104,** 470–486
69. Robinson, R., Carpenter, D., Shaw, M. A., Halsall, J., and Hopkins, P. (2006) *Hum. Mutat.* **27,** 977–989
70. Abramson, J. J., and Salama, G. (1989) *J. Bioenerg. Biomembr.* **21,** 283–294
71. Hurne, A. M., O'Brien, J. J., Wingrove, D., Cherednichenko, G., Allen, P. D., Beam, K. G., and Pessah, I. N. (2005) *J. Biol. Chem.* **280,** 36994–37004